CORROSION BEHAVIOUR OF NICKEL AND MONEL

IN AQUEOUS FLUORIDE MEDIA

by

HUGH D. W. NEY

A THESIS SUBMITTED IN PARTIAL FULFILMENT OF

THE REQUIREMENTS FOR THE DEGREE OF

MASTER OF APPLIED SCIENCE

IN THE DEPARTMENT

of

METALLURGY

We accept this thesis as conforming to the
required standard

Members of the Department of Metallurgy

THE UNIVERSITY OF BRITISH COLUMBIA

February 1964

In presenting this thesis in partial fulfilment of
the requirements for an advanced degree at the University
of British Columbia, I agree that the Library shall make
it freely available for reference and study. I further
agree that permission for extensive copying of this thesis
for scholarly purposes may be granted by the Head of my
Department or by his representatives. It is understood
that copying or publication of this thesis for financial
gain shall not be allowed without my written permission.

Department of ___ METALLURGY ___

The University of British Columbia,
Vancouver 8, Canada.

Date ___ February ___ 1964 ___

ABSTRACT

The corrosion behaviour of nickel and monel in aqueous fluoride solutions was studied by potentiostatic polarization techniques and surface examination of the corroded specimens.

Nickel does not exhibit the usual active-passive transition for $0 <$ pH < 4.0 but corrodes rapidly especially at the grain boundaries. In the range $4.0 <$ pH < 6.5 the nickel polarization curve contains two active regions. Nickel is passive in contact with a fluoride solution with $6.5 <$ pH < 12.0.

Polarization curves of nickel in fluoride solutions of varied pH's and fluoride ion concentrations in the range $4.0 <$ pH < 7.0 revealed that the current as a function of potential in the first active region is independent of fluoride ion concentration but dependent on pH. The currents in the first passive and second active regions are a function of pH and fluoride ion concentration. Surface examinations showed that nickel corrodes at the grain boundaries in the second active region. A mechanism has been proposed which accounts for corrosion in the second active region by F^- adsorption and passivation by either H_2O or OH^- adsorption on the anodically polarized metal surface. A mathematical analysis based on competitive adsorption of these species as a function of electrode potential is shown to be consistent with the experimental data.

Monel corrodes at less than half the rate of nickel at the mixed potential in fluoride solutions with $0 <$ pH < 6.5 due to its larger hydrogen overvoltage. Monel exhibits active-passive behaviour similar to nickel but with the passive current up to 6 times as large.

ACKNOWLEDGEMENT

TABLE OF CONTENTS

LIST OF FIGURES

List of Figures Continued...

LIST OF TABLES

INTRODUCTION

Previous Work

The corrosion resistance of nickel and nickel alloys to fluorine, hydrogen fluoride and aqueous fluorides is well known. A review[1] of materials resistant to fluorine and its compounds states that nickel and monel (70% nickel, 30% copper) are the most versatile. Nickel and nickel alloys are used in uranium fuel diffusion plants, uranium fuel reprocessing plants[2] and in alkylation plants, all of which use fluorine, hydrogen fluoride, or other fluorides, anhydrous or aqueous.

Some qualitative researches have been done on the corrosion of nickel and its alloys in fluorides. Takhtarova and Antonovskaya[4] found monel and nickel to be resistant to $KF.HF$, NH_4F, $NH_4F.HF$, HF in liquid and vapor phases in the absence of oxygen. Of these, hydrofluoric acid was the most corrosive. Both Schussler[5] and Braun[6] found monel to be resistant to aqueous, concentrated HF but that exposure to the atmosphere resulted in severe attack. Braun also found that galvanic coupling with silver and silver solders in the presence of oxygen increased the attack on monel.

Although none of the previous work on nickel corrosion described polarization studies in fluoride solutions, some work has been done on the effect of other halogen ions on the polarization of nickel in sulphates. Turner[7], using galvanostatic polarization techniques[a], found that chloride

---

[a]   This refers to the method of applying a constant external current to an electrode and following the change in electrode potential with time.

ions increased the current that was required to passivate a nickel electrode. This was attributed to the fact that $NiCl_2$ is more soluble than $NiSO_4$ which was suggested to be the first film formed in the passivating mechanism.

More recently, Truempler and Keller[8], using potentiostatic polarization techniques (holding electrode potential constant independent of current and time) studied the affect of Cl^- and Br^- on the passivation behaviour of nickel in sulphate solution. They too found that halogen ions increased the activity of nickel (defined here as the anodic dissolution current of nickel in active potential regions, see Figure 1). The presence of halogen ions also caused a second active region above -300 mV. In both active regions the corrosion process yielded Ni^{++} ions.

Halide ions have also been reported to produce a secondary activity in zirconium, magnesium and aluminium[9] similar to that found by Truempler and Keller except that the electrode did not passivate again. This second active peak resulted in pitting corrosion. The mechanism as explained by Kolotyrkin[10] will be discussed later in reference to the present work. Briefly, he attributes the second active peak to the adsorption of the halide ions due to their polarizability at higher electrode potentials so that they replace the passivating oxygen at random sites. The halide ions cause the nickel to ionize by forming complexes with the nickel atoms. The critical concentration of halide ions is initiated and maintained at the dissolution sites as the halide ions carry the current to them.

Other work has been done on nickel in sulphate electrolytes. Tronstad[11] studied the films on nickel by polarized light. He proposes that the passivity is due to the formation of an oxide film which grows

to a constant thickness of about 40 Å. MacGillavry et al.[12] studied nickel potentials in solutions of various foreign ions. He proposed that dissolution of nickel in the presence of O_2 takes place by the interaction of hydrogen ions with the oxide film.

Vetter and Arnold[13] and Osterwald and Uhlig[14] obtained similar results for the potentiostatic polarization of nickel in sulphuric acid. However, they postulated different mechanisms for the passivating process. Vetter follows Evan's school in proposing that the passivation results from oxide or hydroxide film formation whereas Uhlig maintains that chemisorbed oxygen from water passivates the metal surface.

The question of the mechanism of metal passivation is probably one of definition as much as concept. Evans[15], in suggesting this, has stated that a three-dimensional film is necessary for a metal to remain passive under changing conditions. He readily admits that, upon attaining the Flade potential (E_F in Figure 1) less than a monolayer of oxygen is sufficient to stop corrosion. The monolayer will tend to grow to an oxide film, the thickness depending on the potential and character of the supporting electrolyte.

Bune and Kolotyrkin[16] have used various oxidants in sulphate solutions to show that these produce anodic currents which polarize the nickel in the same way that a nickel electrode can be polarized potentiostatically. They concluded that the dissolution current of nickel is a function of the electrode potential only. This is important as it indicates that metals can be chemically passivated by the addition of oxidizing agents to the corrosive medium.
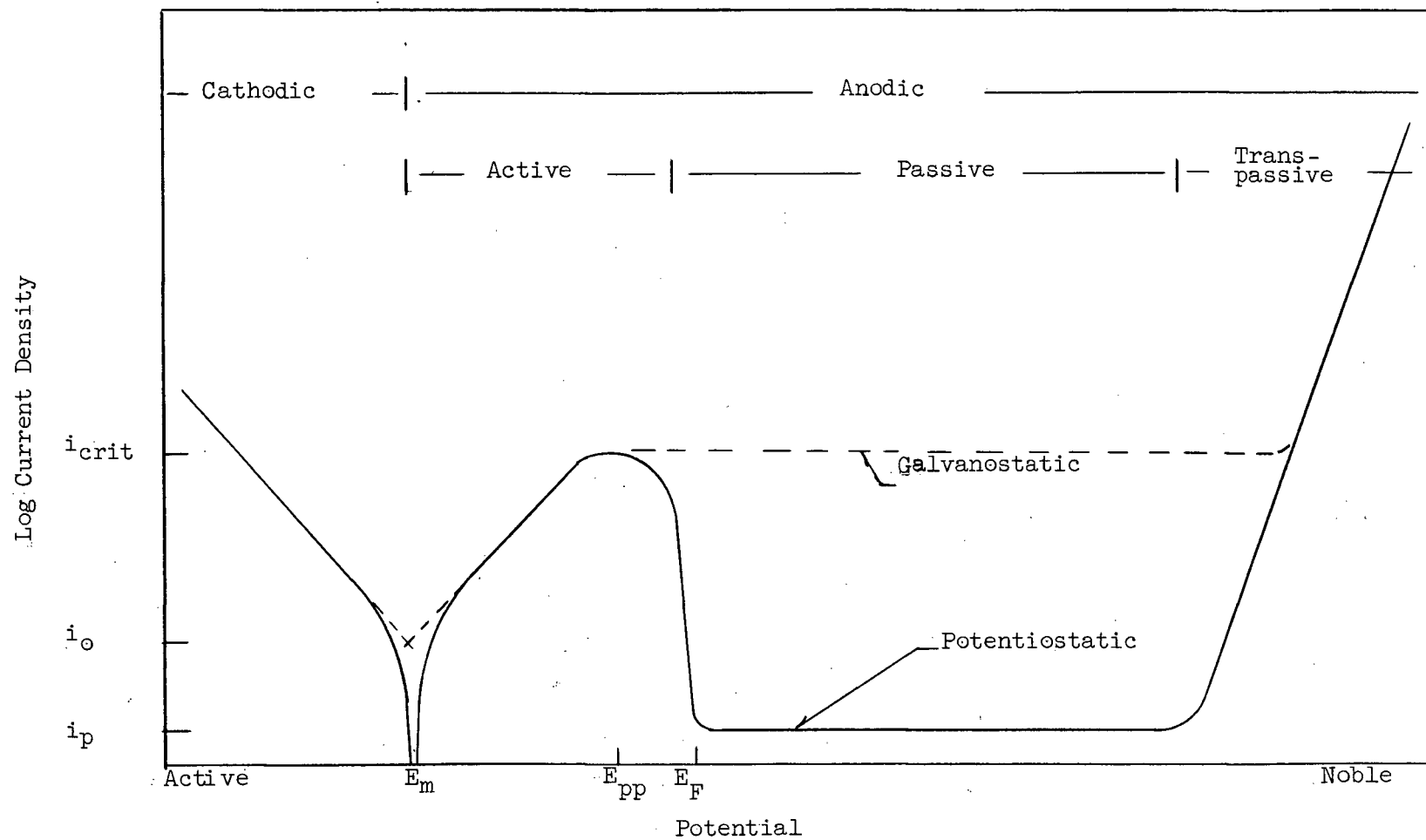
Figure 1. Typical Polarization Curve of a Metal with an Active-Passive Transistion.

Potentiostatic Polarization

Polarization of metals in solution has long been used as a method to elucidate corrosion mechanisms and to determine the possibilities of anodic protection of the metal. However, it is only within the past ten years that potentiostatic techniques have been extensively used. Modern techniques are based on the use of an electronic device called a potentiostat. This instrument detects any variation of the electrode potential with respect to a reference electrode which is in the circuit. The potential is then brought back to the preset value by automatically adjusting the current flowing between the working electrode and an auxiliary electrode (see Figure 7).

Much has been written about potentiostatic polarization methods[17-23]. The essence of these will be briefly summarized here. Potentiostatic techniques are usually applied to the study of passivating electrodes and it is in this connection they will be discussed.

Figure 1 shows typical potentiostatic (a) and galvanostatic (b) curves for a metal showing an active-passive transition. The mixed or rest potential of any electrode in solution (no externally applied current) is that potential at which the rate of the cathodic and anodic reactions occuring on its surface are equal. In many instances the cathodic reaction is

$$2H^+ + 2e^- \longrightarrow H_2 \, ,$$
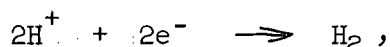
or if oxygen is present

$$1/2O_2 + H_2O + 2e^- \longrightarrow 2OH^- ,$$
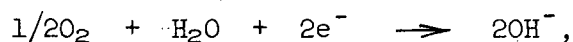
and the anodic reaction is

$$M \longrightarrow M^{++} + 2e^- .$$
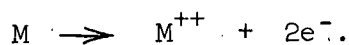
If the electrode is polarized cathodically from the mixed potential by the application of an external current the cathodic reaction predominates and its rate increases with further polarization. Similar considerations apply to anodic polarization. The relation between the logarithm of current and the potential of the electrode is known as the polarization curve.

If the anodic reaction increases as shown the electrode is active. However, on further potentiostatic polarization in the anodic direction the anodic current may fall sharply as the electrode becomes passive. This is because the formation of a protective oxide or hydroxide film becomes kinetically favourable or oxygen is chemisorbed on the metal surface. As long as the passive state persists the anodic potential causes no further increase in current. The corrosion rate is usually controlled by the rate of metal ion diffusion through the passive layer.

At some higher potential in the anodic direction the electrode becomes transpassive (i.e. the current begins to rise steeply) due to film breakdown or the initiation of another anodic reaction. The polarization curve can then be subdivided into a cathodic region and an anodic region with active, passive and transpassive parts.

Certain electrochemical parameters may be determined from the polarization curve which characterizes the metal's corrosion behaviour in that particular medium. By extrapolating the linear portions of the curve in the active region, the corrosion or mixed potentials E_m and the corrosion or exchange current, i_o, are determined by the intersection, Figure 1. The exchange current is the rate of the anodic and cathodic reactions occuring on the electrode surface with no externally applied current. If the anodic

current is the oxidation of the metal to metal ions, then the exchange
current gives the corrosion rate[19].

The slopes of the linear regions (Tafel slopes) are characteristics
of the anodic process, usually metal dissolution

$$M \longrightarrow M^{+n} + ne^-$$
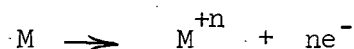
and the cathodic process

$$2H^+ + 2e^- \longrightarrow H_2$$

or

$$1/2\ O_2 + H_2O + 2e^- \longrightarrow 2OH^-$$
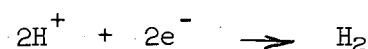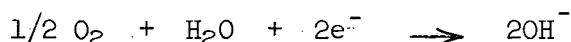
Linear regions of the polarization curve indicate an activation
or concentration controlled reaction, both of which fit the Tafel equation

$$E - E_O = \eta = a + b\ \log\ i$$

where E is the potential of the electrode,
E_O is the reversible potential for the electrode reaction,
η is the overvoltage or polarization,
a and b are Tafel constants, and
i is the current density.

The Tafel equation can be derived from theoretical considerations[24]. For
an activation controlled process it can be shown that

$$b = \frac{2.3\ RT}{\alpha n\ F}$$

and

$$a = \frac{2.3\ RT}{\alpha n\ F}\ \log\ i_O$$

where R is the universal gas constant,
T is the absolute temperature,
n is the number of electrons being exchanged at the activation
barrier
F is the Faraday constant and
α is a factor between o and 1 representing the symmetry of
the activation barrier.

These relationships show that measurement of the Tafel slope permits the estimation of αn. If n is known (e.g. if the rate-determining step is identical to the overall reaction

$$\text{Ni} \longrightarrow \text{Ni}^{++} + 2e^-$$

in which n = 2) then α is obtained. However, n may not be known because the number of electrons taking part per molecule in the rate-determining step is not necessarily identical with the number in the overall reaction. If it can be assumed that α is approximately 0.5, the number of electrons in the rate-determining step may be ascertained. If b becomes infinite then the rate-controlling step is not electrochemical. Thus an examination of the Tafel plot of an electrochemical reaction can sometimes reveal the nature of the rate-determining step.

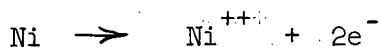Three important parameters from the anodic polarization curve of a metal showing an active-passive transition are the critical anodic current density, i_{crit}, the primary passive potential E_{pp} (the current density and potential at the active maximum) and the Flade potential E_F (the most noble potential at which an electrode will be self-activated after passivation). These indicate the ease of passivation and stability of the passive condition of a metal. Low values of i_{crit} and active values of E_{pp} and E_F lead to ease of passivation. An active value of E_F also indicates stable passivation in unstable environments. A long range of potential through which the metal remains passive and a small passive corrosion rate i_p, enhance the possibilities for protecting the metal by anodic polarization. This can be illustrated by considering different activation-controlled reduction polarization curves when superimposed on the anodic curve. Three such curves with different redox exchange currents are shown in Figure 2.[23]
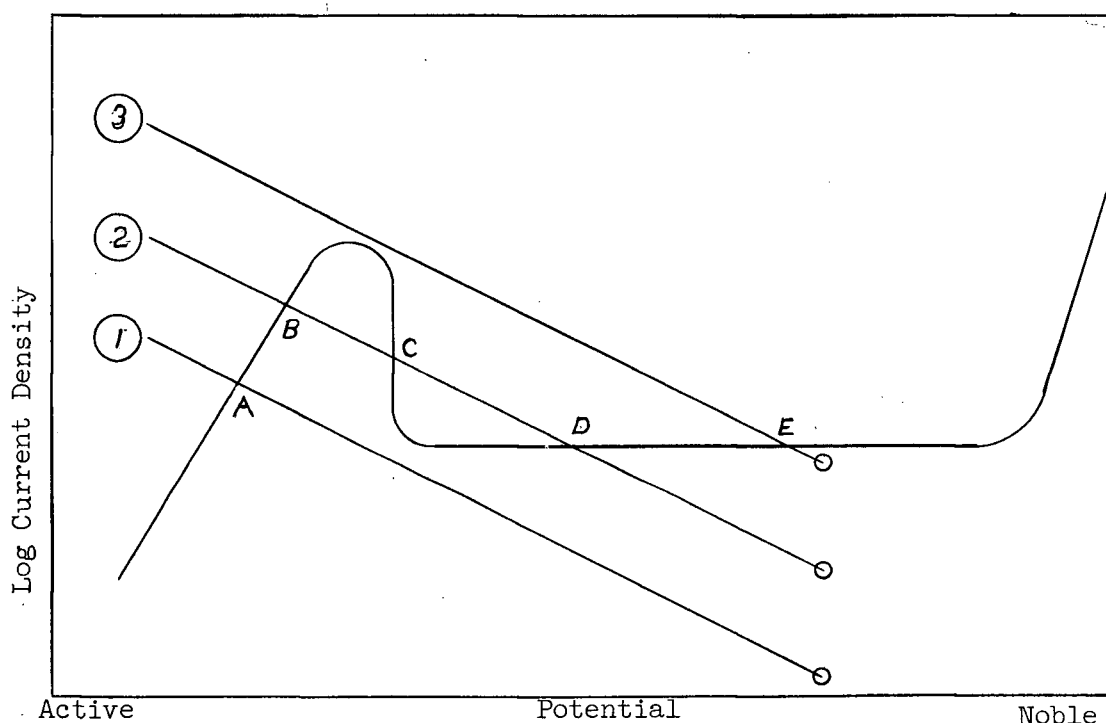
Figure 2. Cathodic Curves with Different Redox Exchange
Currents Superimposed on an Anodic Curve.

For case 1 the rate of oxidation equals the rate of reduction at

point A indicating that the electrode is in the active state (i.e. corrodes

rapidly) at the rest potential. For case 2 however there are three points

where the anodic and cathodic rates are equal. It can be shown that only

points B and D represent stable potentials. Environmental and historical

conditions of the electrode will govern whether the electrode is in the active

or the passive condition or both. In case 3 the electrode is passive and

will corrode at the rate indicated by the passive current. Obviously case

3 represents the most favourable condition for corrosion resistance. This

condition is most easily attained if E_{pp} and E_F are fairly active with respect

to the reversible hydrogen potential and if i_{crit} is small, it is most

stable if E_F is active and the potential range of passivation is extensive

and it is most resistant if the passive current is negligible. Potentio-static polarization of electrodes in conditions represented by the above cases yields curves as shown in Figures 3a, b, and c. (dashed lines indicate cathodic current.)
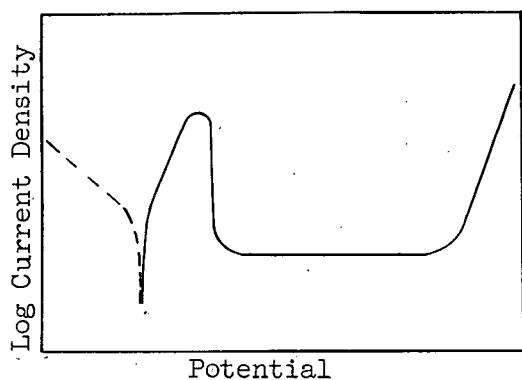
(a) Case 1.
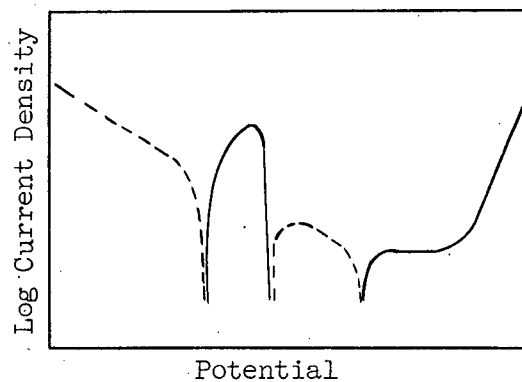
(b) Case 2.
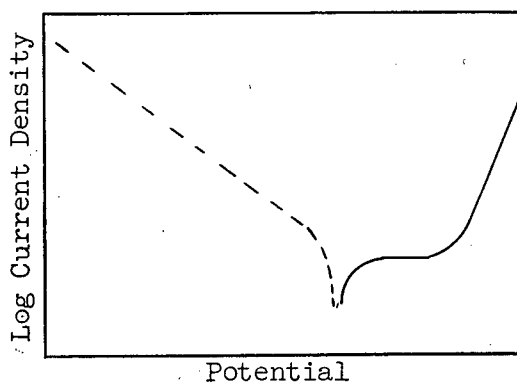
(c) Case 3.

Figure 3. Polarization Curves Showing Effect of Change in Cathodic Redox Exchange Current.

Polarization curves are also useful in indicating the rate-controlling reaction at the mixed potential: that is, they indicate whether the rate of corrosion is cathodically, anodically or jointly controlled and if

in each case the rate-controlling step is electrochemical or physical.
Four cases, in which the rate-controlling step is either electrochemical
activation or diffusion, are illustrated in Figures 4a, b, c, and d.[25]
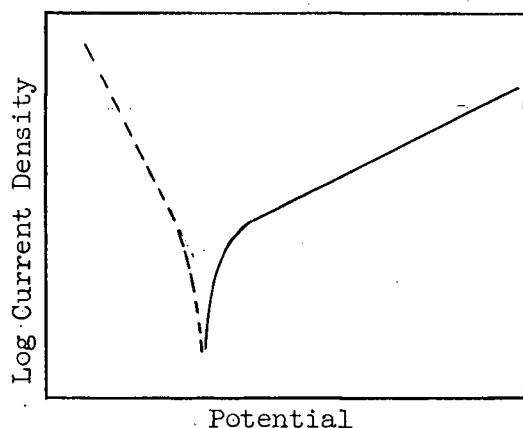
(a) Anodic Activation Control
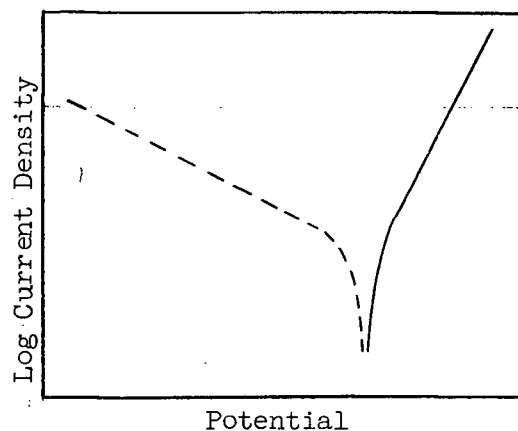
(b) Cathodic Activation Control
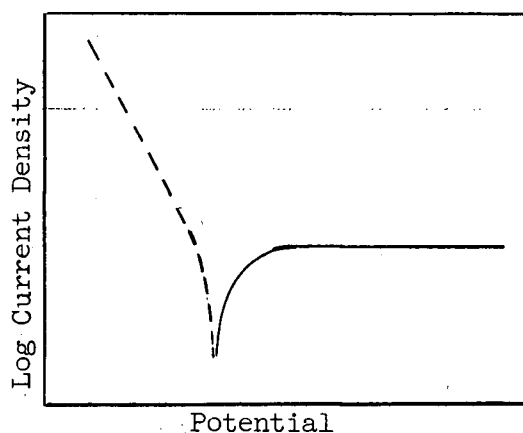
(c) Anodic Diffusion Control
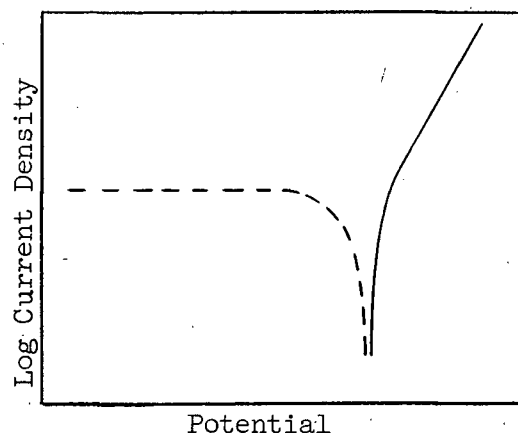
(d) Cathodic Diffusion Control

Figure 4. Anodic or Cathodic Rate Control of the Corrosion
Current.

There are certain drawbacks to the use of polarization curves for
the above purposes. One is that external currents only represent the sum of
all electrochemical reactions occuring at the electrode surface. However,

the reaction which is accounting for all or most of the current is usually known.

The current at a set potential is nearly always time-dependent and may take days to become stable. But with the passage of current and time the condition of the electrode surface and its environment change. Therefore the shape of the curve may greatly depend on the technique used in obtaining the potential-current data[26]. The above-mentioned change in surface condition is especially significant if pitting occurs. Then the anodic current is nearly completely accounted for by the metal oxidation at the pit. Often the cathodic reaction is occuring on the non-corroding areas even when polarized anodically so that the true anodic current is greater than the apparent current[10].

pH-Potential Diagram for Ni-H_2O

The energy relationships of a metal with aqueous environments may be summarized by means of a Pourbaix or pH-potential diagram. The relationships indicate the conditions of corrosion, passivation or immunity. Figure 5. is the pH-potential diagram for nickel in water[27]. The lines represent equilibria between the solid phases and selected concentrations of nickel dissolved in water. These concentrations may be used to define conditions of passivity and nobility, and it has become a convention to use 10^{-6} M dissolved metal ions as the arbitrarily defined limit of corrosion.

With fluorides in the system the diagram is changed very little except that $NiF_2 \cdot 4H_2O$ is thermodynamically stable with respect to Ni^{++} at concentrations greater than 10^{-6} M. The boundaries of its stability are very similar to Ni^{++} in pure H_2O. However in most circumstances it does not form an adherent film on the nickel surface. The effect of fluoride is therefore disregarded in discussing the pH-potential diagram.
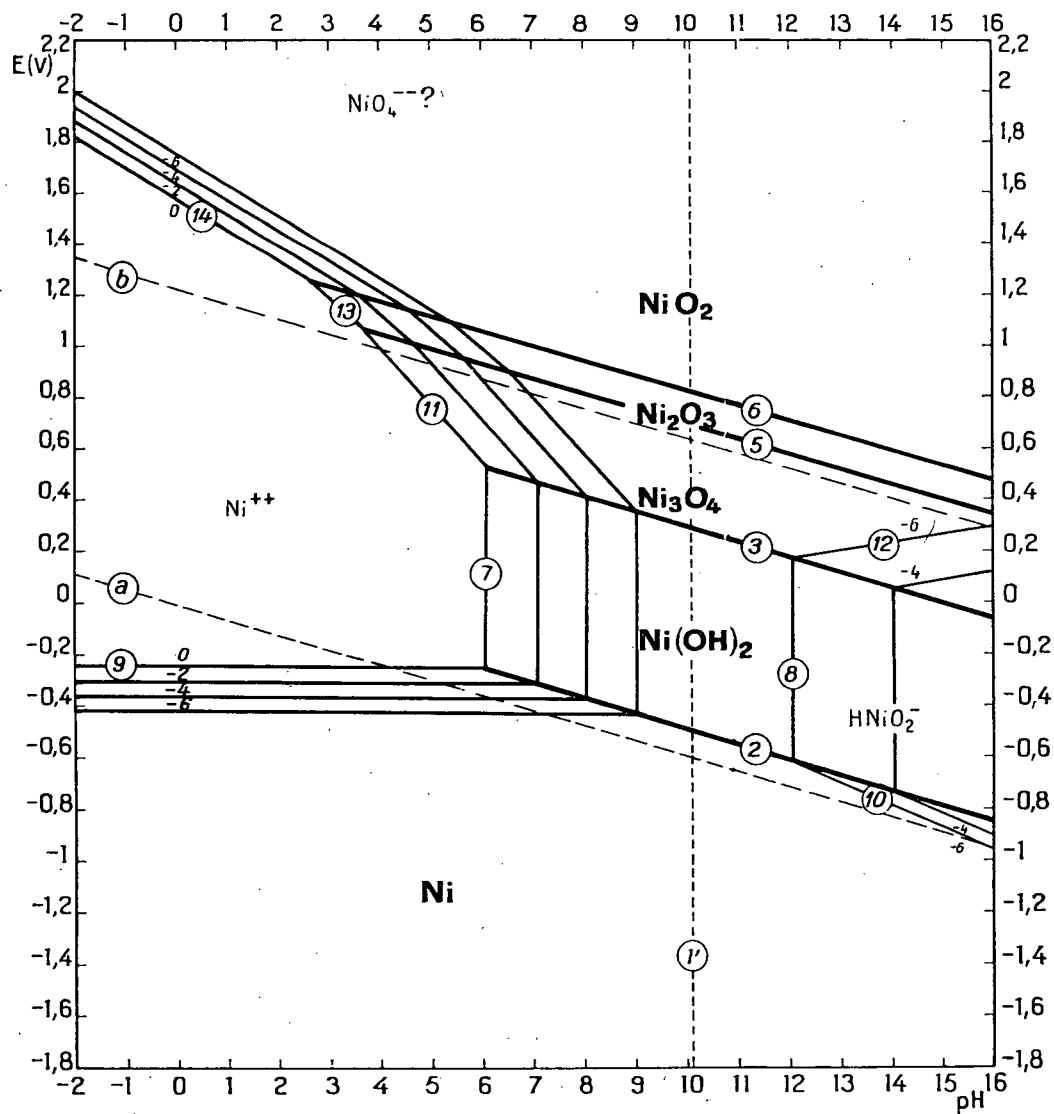
Figure 5. Nickel-Water pH-Potential Diagram

Nickel in a solution containing 10^{-6} M Ni^{++} should be passive at any potential in the pH range 9-12, according to the pH-potential diagram. This is because Ni (OH)$_2$ or higher oxides are stable in that they have solubilities below 10^{-6} M and are considered to form a protective film. Ni(OH)$_2$ forms at the rest potential so that associated polarization curves should show little or no activity. At pH $<$ 9 nickel would not be expected to passivate. However, this is not always the case as water molecules or hydroxide ions may be adsorbed at potentials above the rest potential, and initiate the formation of a hydroxide film. In this case the polarization curve usually shows an active region, the extent of which may depend on the ions in solution. Nickel should corrode at still higher potentials in this pH region due to the formation of hexavalent nickel as NiO_4^{2-}. Nickel would also be expected to corrode in aqueous solutions with a pH $>$ 12 to form NiO_2H^- instead of the passivating Ni(OH)$_2$.

Throughout the pH region 0 to 12 higher oxides of nickel are stable at sufficiently noble potentials. These may form an adherent film but if they are good electronic and ionic conductors they will not be protective. They will probably be good ionic conductors if they have a defect structure, which the NiO$_2$ lattice is known to have[28].

Purpose and Scope of the Present Investigation

The purpose of this investigation was to examine polarization curves for nickel and monel in solutions of varying pH and fluoride content for evidence of corrosion-resisting properties and of possible corrosion mechanisms of these metals in this range of environments. Indications were also sought for methods of improving corrosion resistance in those solution compositions where corrosion rates may be considered excessive.

Initial experiments entailed polarization studies at widely
varying pH in buffered electrolytes. The curve in a fluoride electrolyte
of pH = 6.2 showed a second active peak which was reported but not explained
by Truempler and Keller[8] in chloride solutions. Further studies were
conducted in an attempt to explain this anomaly. These consisted of
polarization studies at different fluoride and hydrogen ion concentrations,
current-time curves at constant potential and surface examinations of
corroded specimens. Polarization curves were also obtained for nickel
in chloride solution, to determine any difference in corrosion behaviour
with other halide ions, and in nitrate solution as a halogen-free reference.

Potentiostatic curves for monel in fluorides and chlorides were
obtained in an attempt to relate the behaviour of monel and nickel.

APPARATUS AND EXPERIMENTAL

Electrochemical Cell and Electrical Apparatus

The highly corrosive nature of fluorides greatly limited the materials and thus the design of the test cell. Tetrafluoroethylene (Teflon) was used because of its inertness and high temperature (500°F) strength. The cell designed for the present work (Figure 6) is similar to a cell described by Weininger and Grams[29] and contains all the essential elements, which are

1. working, auxiliary and reference electrodes

2. circulating electrolyte

3. gas saturation inlet and outlet

4. provision for heating and temperature control.

The cell design also lends itself to ease of changing the working electrode and electrolyte.

All parts are machined from rod, bar and tube stock Teflon supplied by the Crane Packing Company. The cell consists of a 2 inch I.D., 3 inch O.D. Teflon cylinder (a), with disks or electrode holders above (b) and below (c). The cell is sealed by O-rings and clamped together by bearing plates and threaded rods, (p).

The working electrode (d) is wrapped with Teflon tape and drawn into place by tightening the nut at the end of the stainless steel bolt (r) that also acts as an electrical connection and is insulated from the bearing plate by a bakelite washer. The auxiliary electrode (f) is a circular disk of the same metal as the working electrode, and is held in place by the stiff copper wire (h) that is soldered to it. The reference electrode (e) is
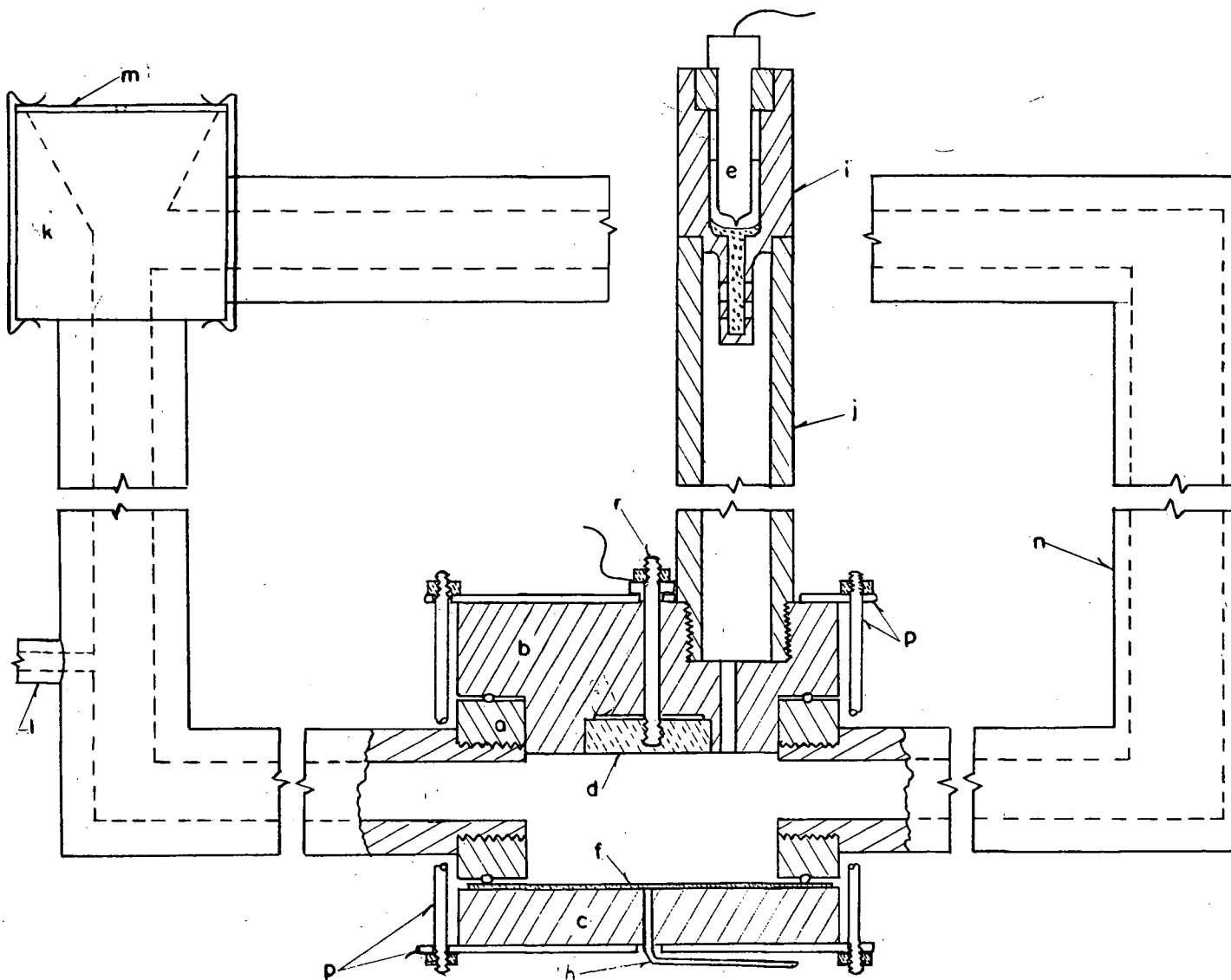
Figure 6. Electrochemical Corrosion Cell

located in a Teflon insert (i) filled with saturated KCl. The bottom of

the insert is perforated and filled with agar agar gel of saturated KCl

which is in contact with the electrolyte in tube (j). A small hole in

the top of the cell next to the working electrode allows electrolyte into

this tube.

The electrolyte is poured into the funnel at (k) and circulates

by the gas lift at (l). This provides circulation through the cell and

parallel to the electrode faces. This also saturates the electrolyte with

the particular gas used, in this case nitrogen ($< 0.7\%$ O_2) from compressed

gas tanks supplied by Canadian Liquid Air Company. A Teflon sheet (m)

with a small hole in it is clamped over the funnel and maintains small

positive pressure of the saturating gas over the electrolyte.

This cell has the advantage of being flexible in use and simple

in design but does not permit the cell reaction to be observed.

A schematic diagram of the electrical system is shown in Figure 7.[39]

The potentiostat is a Duffers Model 600. Current is supplied from a 12 volt

center-taped Delco car battery and is measured by a Simpson Model 29MC

50 microampere (μA) ammeter to which is added shunts and a shorting type

reversing switch giving full scale readings of 50 μA, 200 μA, 500 μA, 2 mA

5 mA and 20 mA in both directions. The ammeter is in the auxiliary electrode

lead. The potential between the saturated calomel reference electrode and

the working electrode is measured by a Model 7569p Pye Potentiometer using

a Beckman Model G.S. pH meter as a high sensitivity, high impedance null

detector.
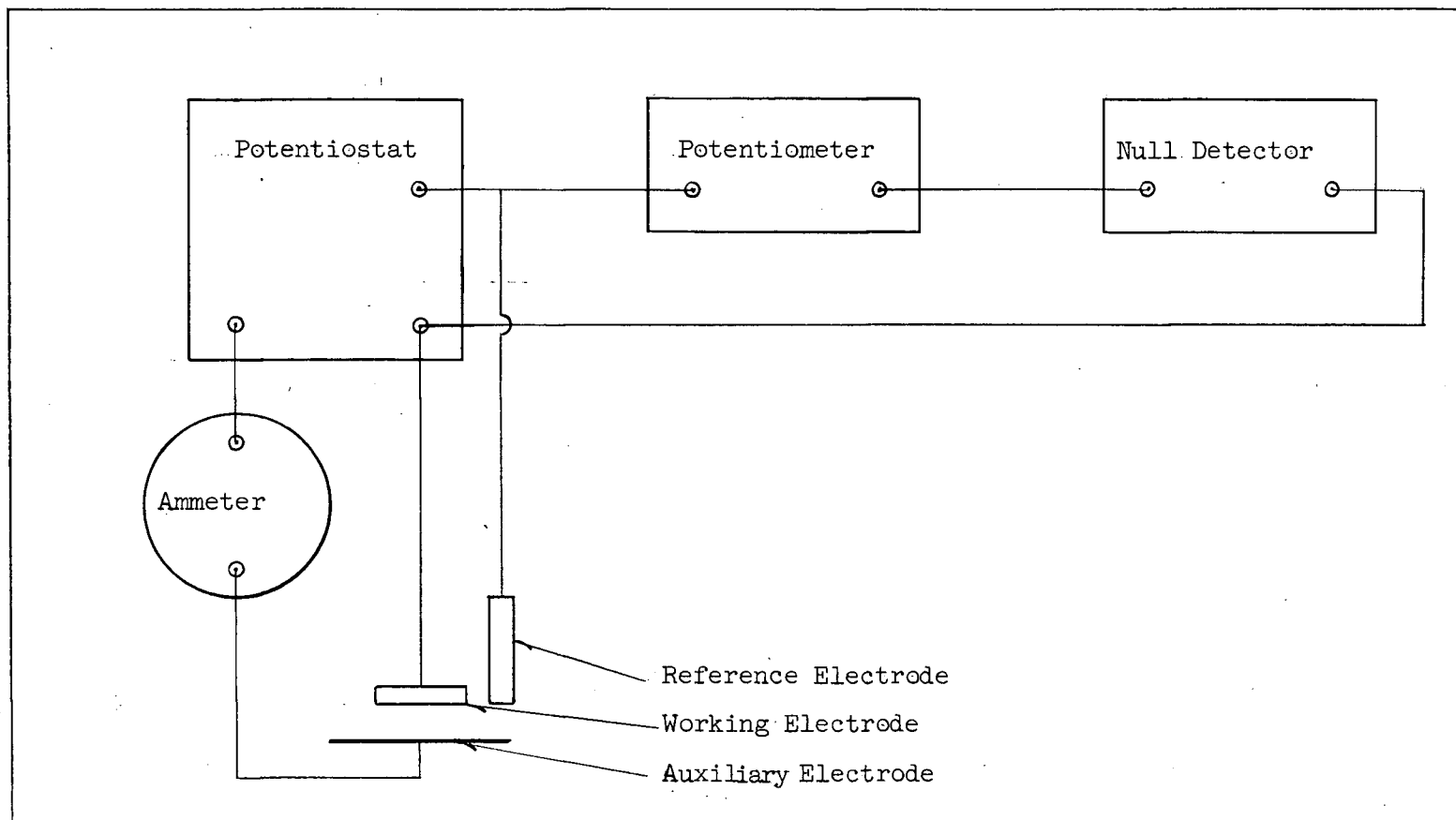
Figure 7.   Schematic Diagram of Electrical Apparatus

Unfortunately the potentiostat required frequent maintenance service. To overcome delays caused by breakdowns, a "classical" potentiostat was also used. It consisted of two 2.2 volt Hart D.H.S. 15 glass wet cells in parallel, from which a polarizing current is drawn by adjusting an Ohmite three-pole 8.5 ohm variable resistor. The current was measured by the modified Simpson ammeter but in order to follow the potential drift more closely a Beckman "Zeromatic" pH meter was used for measuring the potential. This has the required high impedance but much lower sensitivity ($\pm$ 10 mV).

Materials

Electrodes (5 cm^2 in area) were machined from rod supplied by A.D. MacKay Inc. with stated purities of 99.9% for both monel and nickel. When impurities were suspected to be present in the nickel, it was analyzed, with the following results:

Sulphur	0.015 %
Carbon	0.030
Iron	0.040
Copper	0.150
Cobalt	0.350

The monel sheet for the auxiliary electrode was also supplied by A.D. MacKay, Inc. The nickel auxiliary electrode was supplied by Mr. V. N. Mackiw of Sherritt Gordon Mines Limited.

All reagents used in the electrolytes were Baker and Adamson reagent grade chemicals diluted in distilled water. The electrolytes were buffered with phosphate or succinate.

Polarization Curves

The corrosion specimen was mounted in the test cell after polishing with 1/2 grit emery paper and cleaning with Chlorothane*. The specimen was aged during nitrogen saturation of the electrolyte for about 1/2 hour and then cathodically reduced for 1/2 hour to remove oxide film. Potential settings were made increasingly anodic beginning from this cathodic region in 10 to 100 mV increments. At each setting initial current readings were made followed by at least one additional reading after 5 or 10 minutes to detect time-dependent current variations. The pH of the electrolyte was measured with short-range Hydrion pH paper before and after each run. The specimen was retained for subsequent examination of the surface.

Curves were obtained for nickel and monel in fluoride solutions at widely varied pH. Most work was done on nickel in fluoride media in the pH range of 4.0 to 7.0 because under these conditions secondary activation was evident. Curves were also obtained in sodium nitrate solutions as a reference and in sodium chloride solutions for comparison.

Several experiments were made with nickel in fluoride solutions at pH = 6.2 to determine the time-dependence of current at potentials corresponding to selected parts of the polarization curve. The growth of a protective film can usually be interpreted from decaying current values. In these experiments the corrosion specimens were left at the selected potentials for one or more days during which time current readings were recorded at intervals. Experimental conditions for all runs are summarized in Table I.

---

*   1,1,1 - trichloroethane

TABLE I.

Experimental Conditions

Experiment Number	Anode Material	Electrolyte	Concentration	Buffer	pH
8	Nickel	NaF	0.39	Phosphate	4.0
10	Nickel	NaF	0.42	Phosphate	11.3
11	Nickel	NaF	0.45	NaOH	>12
12	Nickel	HF	0.1	HF	1.0
13	Nickel	HF + NaF	0.38	Phosphate	5.8
14	Nickel	NaNO$_3$	0.08	Phosphate	6.0
15	Nickel	NaF	0.42	Succinate	5.2
16	Nickel	HF	0.08	Phosphate	2.2
17	Nickel	NaF	0.41	Succinate	6.0
18	Nickel	NaNO$_3$	0.083	Succinate	4.8
19	Nickel	NaCl	0.42	Phosphate	4.9
20	Nickel	NaCl	0.2	Phosphate	6.1
21	Nickel	NaF	0.042	Phosphate	6.2
22	Nickel	NaF	0.21	Phosphate	6.2
23	Nickel	NaF	0.29	Phosphate	6.2
24	Nickel	NaF	0.42	Phosphate	6.2
25B	Nickel	NaF	0.42	Phosphate	6.2
26	Nickel	NaF	0.42	Phosphate	6.2
27B	Nickel	NaF	0.42	Phosphate	6.2
28	Monel	NaF	0.42	Phosphate	6.0
29	Monel	HF + NaF	0.30	-	4.1
30	Monel	NaF	0.42	Phosphate	11.2
31	Monel	NaCl	0.42	Phosphate	4.0
32	Nickel	NaF	0.42	Phosphate	7.0
33	Nickel	NaF	0.42	Phosphate	5.4
34B	Nickel	HF	0.1	-	1.0
35B	Nickel	NaF	0.42	Phosphate	6.2
36B	Nickel	NaF	0.42	Phosphate	6.2
37B	Nickel	NaF	0.42	Phosphate	6.2
38B	Nickel	NaF	0.42	Phosphate	6.2
39B	Nickel	NaNO$_3$	0.1	Phosphate	6.0
40B	Nickel	NaF	0.42	Phosphate	6.2

B indicates current-time experiments.

Surface Examination

The surfaces of all corroded specimens were examined under a binocular microscope for characteristics peculiar to the corrosion system. Specimens corroded at constant potential over extended times were particularly significant. Micrographs were made of these, using a Reichert microscope and Polaroid camera.

RESULTS AND DISCUSSION

Nickel specimens polarized in 0.08 M HF at pH = 2.2 and in

0.42 M NaF at pH = 6.2 and 11.3 each buffered by phosphate gave polarization

curves as shown in Figure 8, 11, and 22 respectively. These curves show

three distinct types of behaviour of nickel in fluorides as a function

of pH.

Nickel in Acid Fluoride Solutions

The curve at pH = 2.2 and another which was done in unbuffered

0.1 M HF at pH = 1.0 show that nickel does not passivate in the presence of

fluoride ions at low pH. In contrast, Vetter[13], Uhlig[14] and Bune[16] found

that nickel passivates on attaining a potential of about -90 mV in sulphuric

acid solutions.

The mixed potentials[*] are plotted versus pH with other data for

nickel in phosphoric and sulphuric acid solution, Figure 9. The value

of 310 mV at pH = 2.2 is intermediate between the mixed potentials in 1 N

sulphuric acid and 0.1 M phosphoric acid. Presumably these foreign ions

have some effect on the reactions on the nickel electrode surface. The

exchange current was determined to be about 50 $\mu A/cm^2$, indicating a fairly

high corrosion rate of 130 mdd or 0.02 ipy.

No time-current experiments were done using this system.

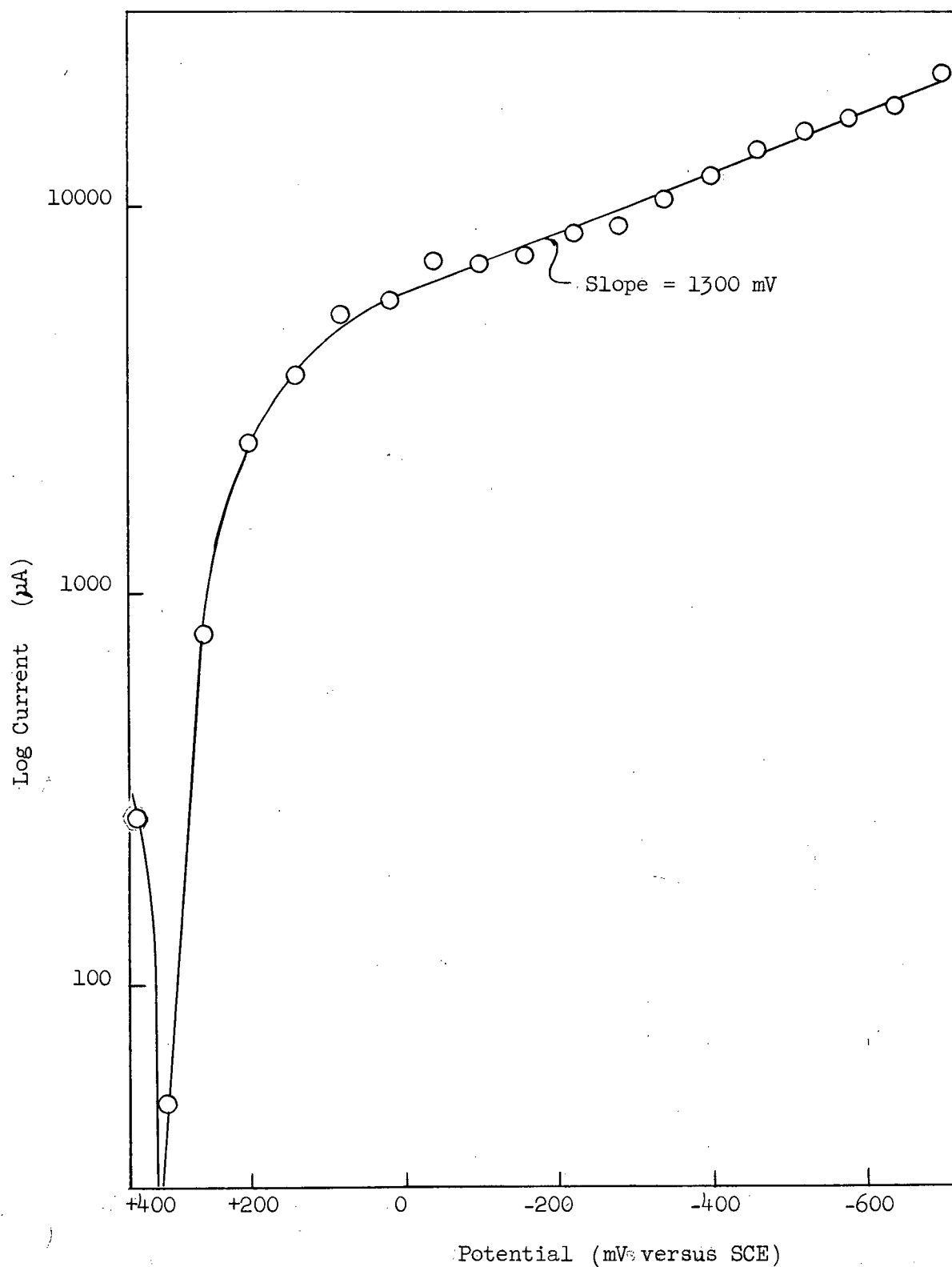[*] See Appendix I for Calibration of Potentials

Figure 8.   Polarization Curve of Nickel in 0.08 M NaF
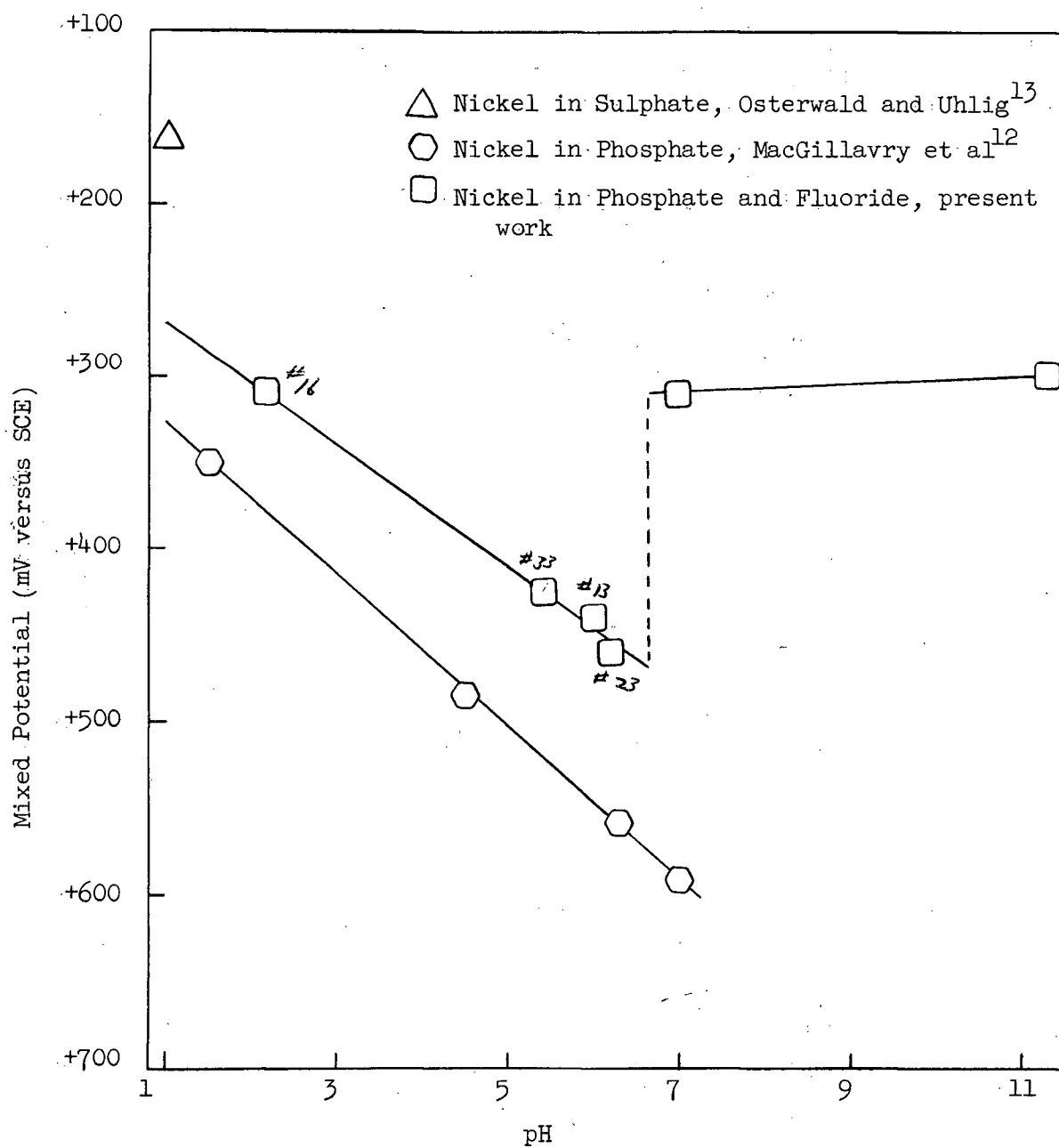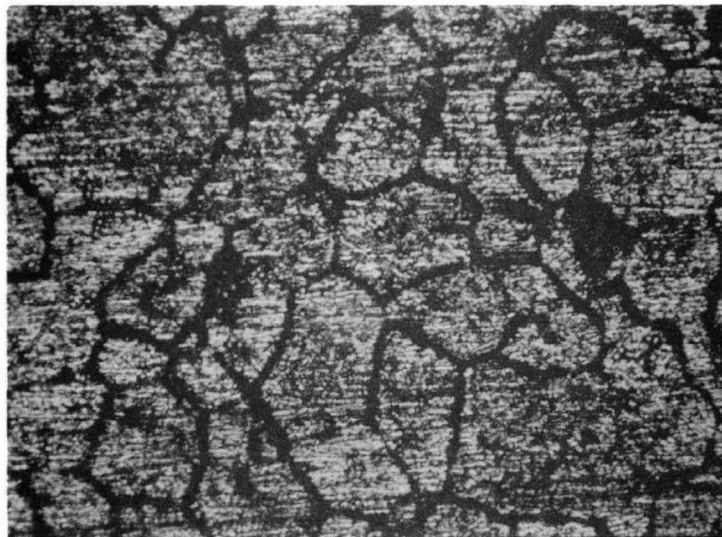Solution at pH = 2.2 *Run* #24

Figure 9. Mixed Potential versus pH

In making the readings for this polarization curve it was noted that the change in current with time was small except for the potential region from + 100 to 0 mV where there may have been some film growth.

Optical examination of the specimen polarized in the phosphate-buffered solution showed interference colours which may indicate film formation. The micrograph, Figure 10a. shows extensive intergranular corrosion. The mechanism of the corrosion which preferentially attacks grain boundaries will be discussed later in relation to the results of nickel corrosion in neutral fluoride solutions. Another specimen was corroded in 0.1 M HF with no applied potential for 1 day. The micrograph Figure 10b. shows extensive pitting corrosion and no general corrosion or film formation between the pits. Obviously, the anodic areas are stationary producing pits while the cathodic reaction occurs on the rest of the surface. From these observations it is evident that nickel is subject to extensive corrosion by fluorides at low pH independent of the applied potential.

Nickel in Neutral Fluoride Solutions

Figure 11 shows that nickel is active in contact with a solution containing fluorides at pH = 6.2. On raising its potential nickel has a typical active-passive transition. Further in the anodic direction there is a second active region similar to that found by Truempler and Keller[8] in sulphate solutions containing chlorides and bromides. This behaviour was not found by Vetter[13] or Uhlig[12] working with nickel in pure sulphates.

(a) At noble potentials pH = 2.2

X 300
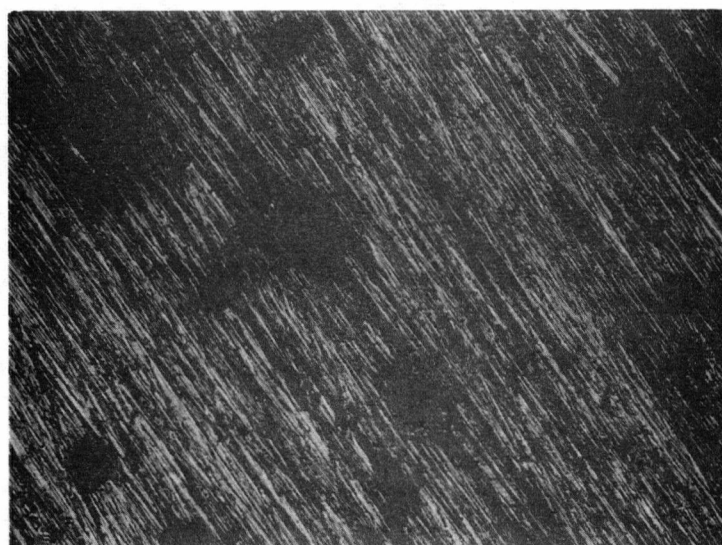
(b) At mixed potential pH = 1.0

X 300

Figure 10. Surfaces of Nickel Corroded in Fluorides at
Low pH

Figure 11. Polarization Curve of Nickel in Fluoride
and Nitrate Solution at pH = 6.2 *Run #24*

The cathodic region, the exchange current, the mixed potential and the first activation peak are functions of pH only. It was not possible to obtain an accurate value of the exchange current because the Tafel plot is n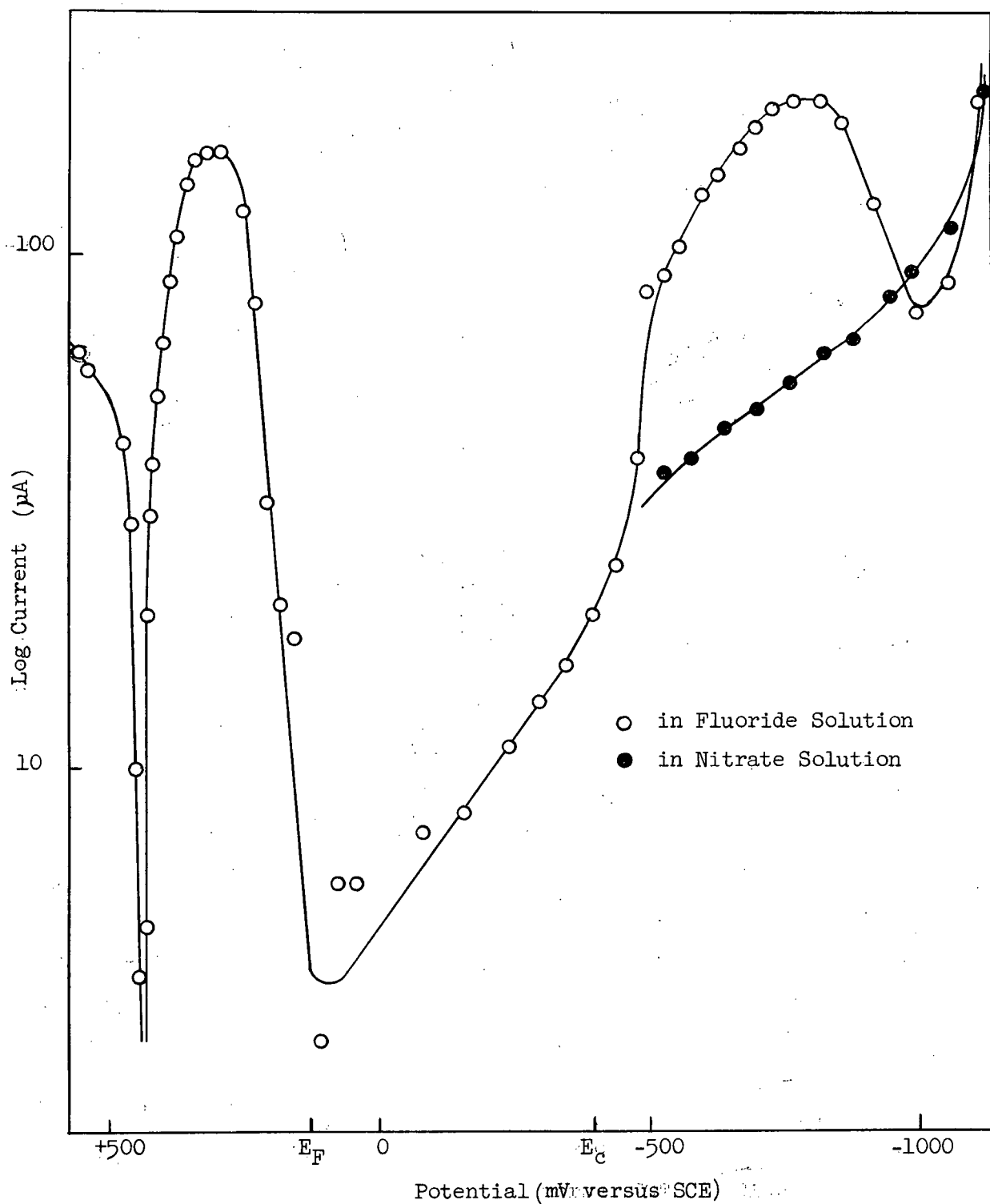ot linear and therefore does not permit accurate extrapolation to the mixed potential. This is illustrated in Figure 11. However an approximate value was obtained by extrapolating the cathodic curve to the mixed potential. Figure 12 is a plot of the estimated exchange current versus pH at varying fluoride ion concentrations. This indicates that nickel becomes fairly passive in fluoride solutions above pH 6.5. The exchange current at pH = 7.0 is 0.3 $\mu A/cm^2$ which corresponds to a corrosion rate of 0.17 mdd or 27 X 10^{-6} ipy.

At low pH's the mixed potential E_m follows the equation

$$E_m = 0.290 + 0.050 \ pH$$

as shown in Figure 9. The abrupt change in potential at about pH = 6.5 is due to a change from activation to ohmic overvoltage of the anodic reaction with the passivation of the electrode. Two experiments (Nos. 15 and 17) using succinate as a buffer gave much more active mixed and Flade potentials, probably because nickel complexes with succinate which is a chelating ion.

The passivation of nickel in aqueous solution at pH = 6.5 is not predicted by the pH-potential diagram. Even if the concentration of Ni^{++} in solution is 10^{-4} M, or 1.5 mg of dissolved nickel, the nickel would not be expected to form a hydroxide film until a pH of 8.0 is attained.

The critical anodic current for passivation is not affected by widely varying fluoride ion concentrations at constant pH as shown by ex experiments numbered 14, 21, 22 and 23. The critical anodic current is
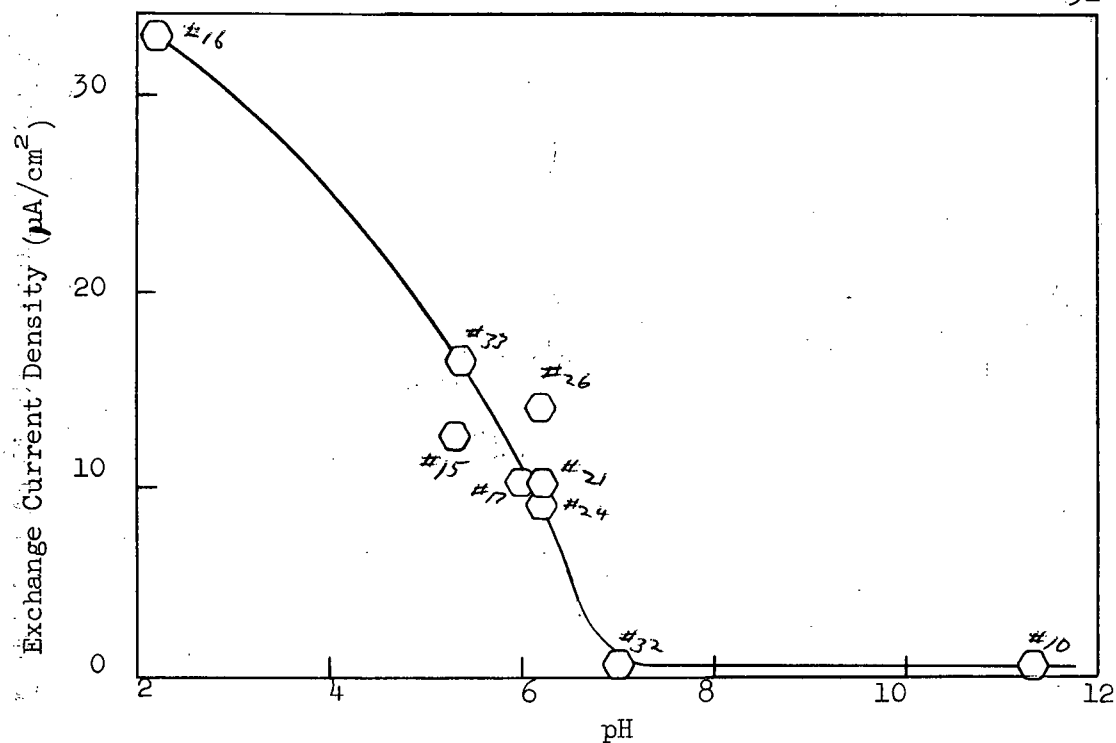
Figure 12.   Exchange Current versus pH
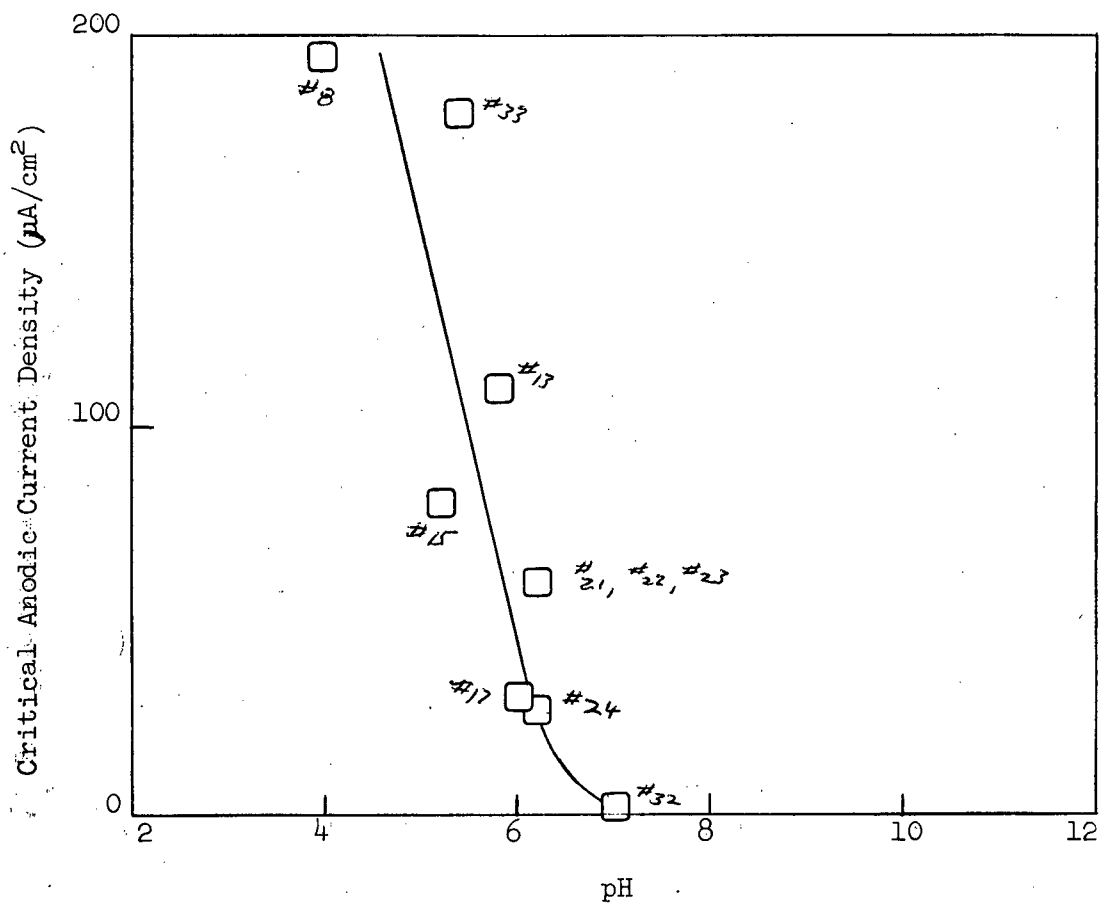
Figure 13.   Critical Anodic Current Density versus pH

$60 \mu A/cm^2$ in each case. On the other hand Truempler and Keller[8] found

that an addition of 0.05 M of chloride ion increased the critical anodic

current from 30 mA/cm^2 to 100 mA/cm^2. However, the critical anodic current i_c

is definitely a function of pH as shown in Figure 13.

The Flade potential follows the equation:

$$E_F = - 0.240 + 0.065 \text{ pH}$$

which compares with the relation given by Uhlig as:

$$E_F = -0.120 + 0.059 \text{ pH}$$

The presence of fluoride ions in solution lessens the resistance

of passivated nickel to corrosion. This effect is increased with increase

in hydrogen ion concentration as illustrated in Figure 14, where pF is the

negative logarithm of fluoride ion concentration. In contrast, changes

Figure 14. Minimum Passive Current Density versus pF + pH.

in pH have little effect on the passivating characteristics of nickel in
sulphuric acid[13, 14].

Current-time curves shown in Figure 15, (a) and (b) indicate
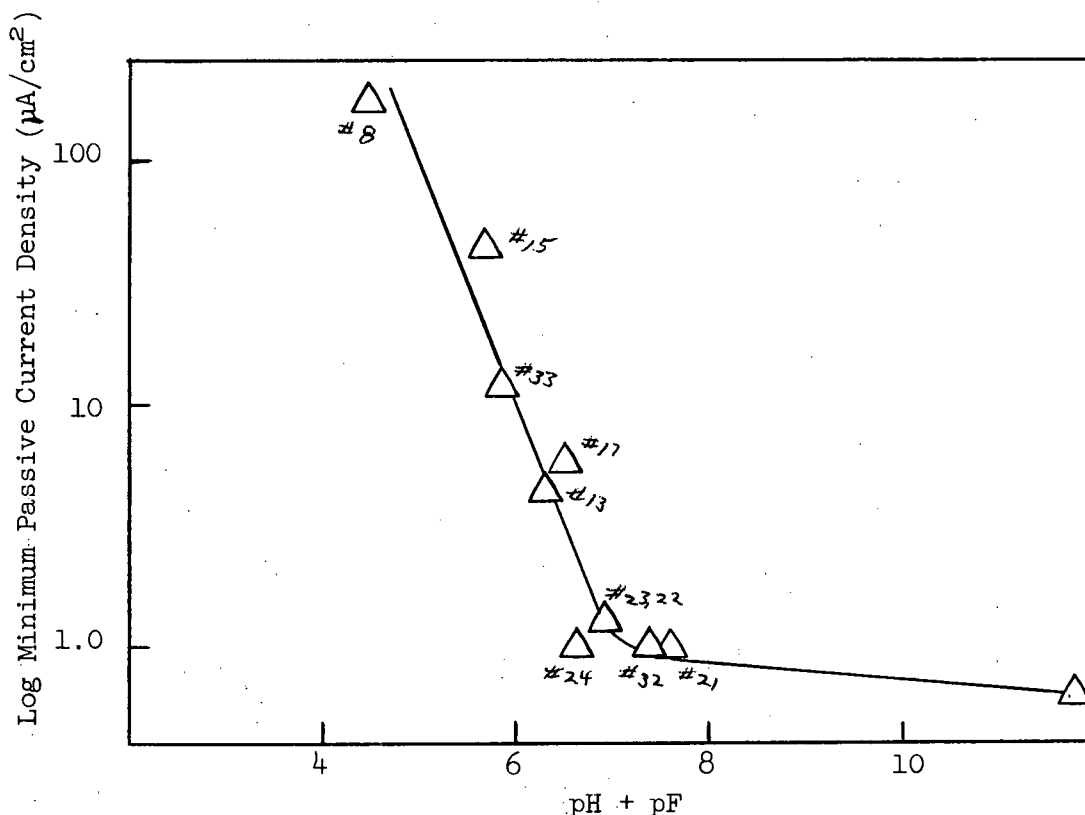film growth in the passive region. Curve (a) at +200 mV gives a final
current density of about 0.5 $\mu A/cm^2$ after 2 hours as compared to the value
of 8 $\mu A/cm^2$ after 5-10 minutes indicated on the polarization curve. This
emphasizes that the polarization curve current readings in this region are
far from the steady-state values. The gradually sloping curve in the active-
passive transition may be more accurate as a vertical line on the basis of
final steady-state currents. The final current at +200 mV is less than the
final current at -150 mV, curve (b). This agrees with the trend shown in
the polarization curves, for the current to increase with the applied potential
in the passive region.

Figure 16 (a) and (b), and Figure 17a, show photomicrographs of
nickel specimens corroded at constant potentials in 0.42 M sodium fluoride
solution at a pH of 6.2. The specimen corroded at the mixed potential for
1.25 days, Figures 16a, shows a large amount of general corrosion which has
nearly obliterated the polish striations. This confirms an expected high
rate of corrosion suggested by the exchange current measurement. The specimen,
corroded in the active region at a potential of +300 mV for 1 day, Figure 16b,
is characterized by both pitting and general corrosion. Figure 17a, is the
surface of a specimen corroded in the passive region for 1.75 days. This
shows less general corrosion. Nevertheless corrosion is still apparent,
while another specimen, Figure 17b held in the passive region with nitrate
replacing fluoride as the electrolyte shows no corrosion. This confirms that
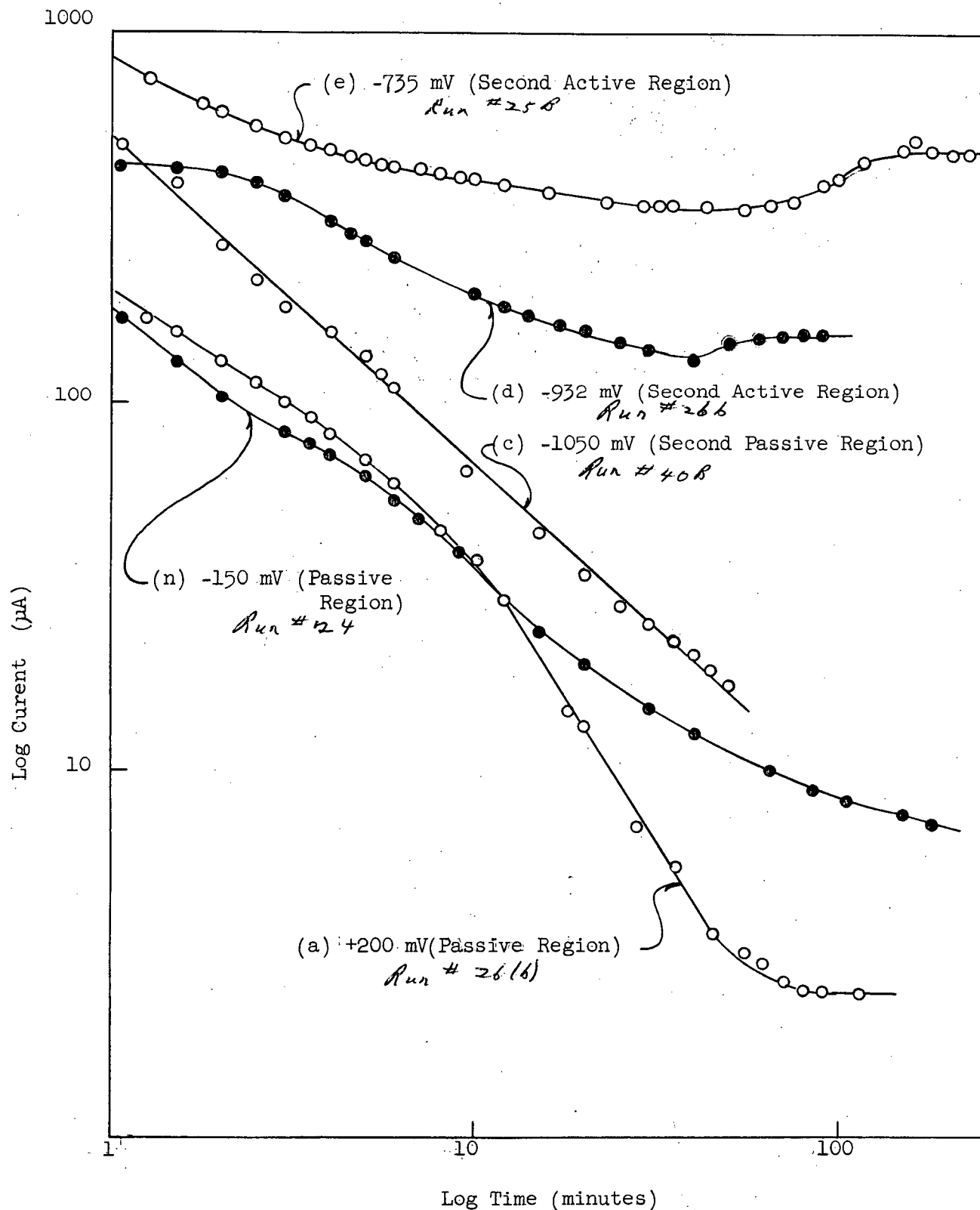
Figure 15. Current-Time Curves at Selected Regions of
Nickel Polarization Curve in 0.42 M NaF Solution
at pH = 6.2
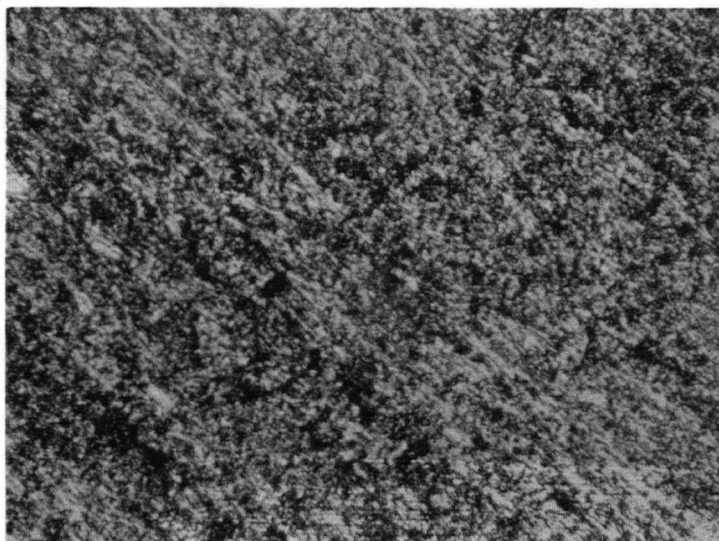
(a) At the mixed potential

X 300
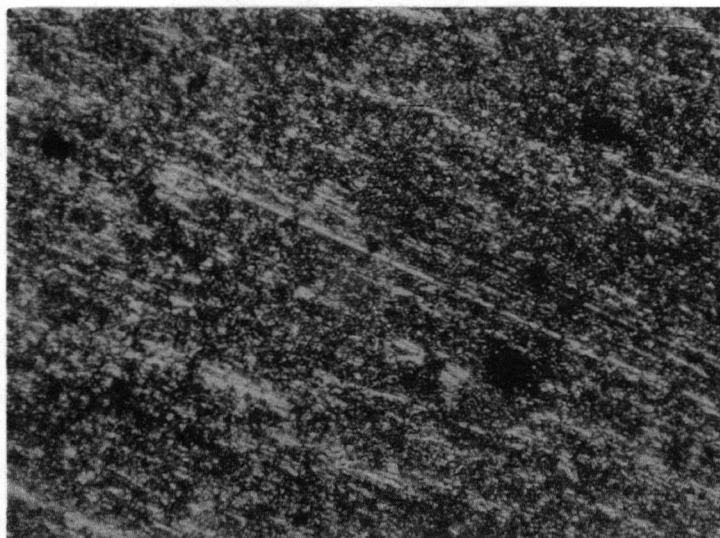
(b) At the active peak, +300 mV.

X 300

Figure 16. Surfaces of Nickel in the First Active State
Corroded in Fluoride Solutions at pH = 6.2
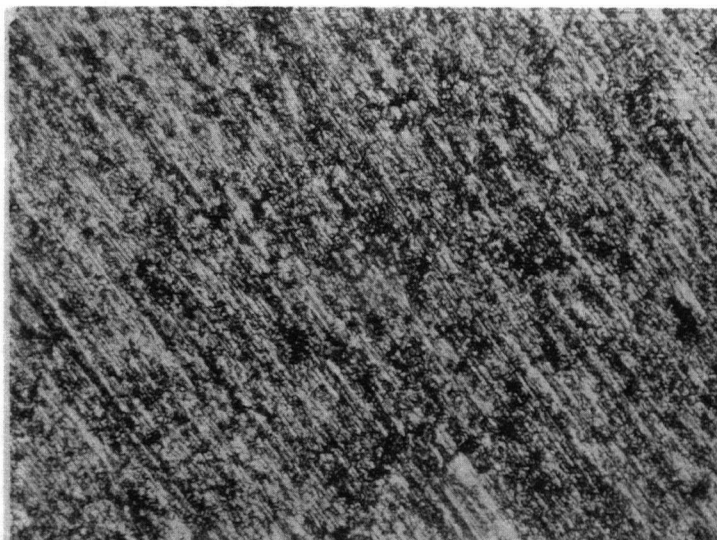
(a) At -150 mV in 0.42 M NaF

X 300
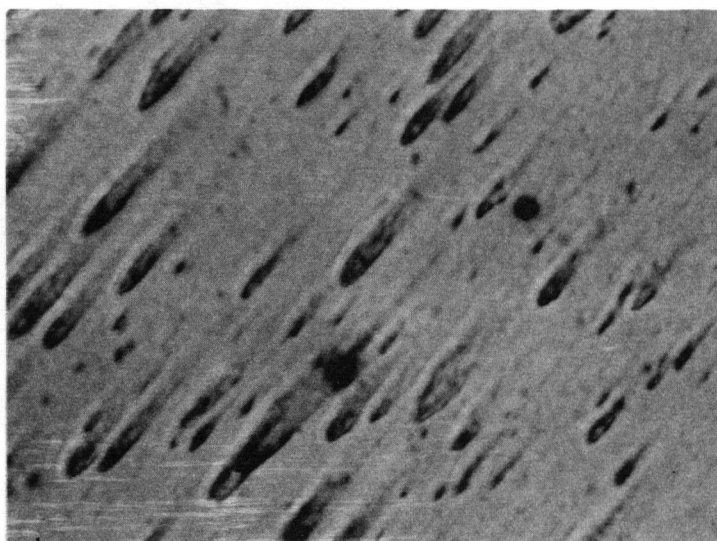
(b) At -200 mV in 0.1 M NaNO₃ (Comet-like
    marks are polish striations)

X 300

Figure 17. Surface of Nickel in the Passive State
            Corroded in Solutions of pH = 6.2

fluoride ions cause nickel to corrode even when apparently passive. The
mechanism whereby fluoride produces this corrosion is not clear. Possibly
fluoride ions are incorporated into the lattice of the hydroxide film
causing it to become an ionic conductor. Alternatively, fluorides may
cause the hydroxide film to dissolve by complexing with the nickel ions
in the lattice of the film.

The fact that fluoride causes corrosion of nickel in the passive
state helps explain the photomicrograph of nickel corroded in the active
state, Figure 16b. U. F. Franck[30] has explained pitting corrosion in the
active state as being due to the existence of active and passive sites on
the same polarized electrode. The difference in potential is caused by
electrolyte resistance. Thus the pits are presumed to be active sites and
the areas of general corrosion are "passive" sites.

Both position and extent of the second active region are functions
of fluoride and hydrogen or hydroxide ion concentrations. The potential
of the active peak, Figure 18 and the logarithm of the current at the peak,
Figure 19, are plotted as functions of pH plus pF. In both cases the
dependence appears to be linear. The potential at the initiation of the
second active region is plotted versus pH plus 2pF, in Figure 20. This
seems to give the best linear fit of the data. Figure 21 is a plot of the
positive Tafel slope of the second active region versus pH plus pF. The
latter indicates a change in the rate-controlling step at a pH plus pF equal
to 6.5 since below this value the Tafel slope is constant of 135 mV, giving
an α n value of 0.45, while at higher values the Tafel slope increases
sharply.
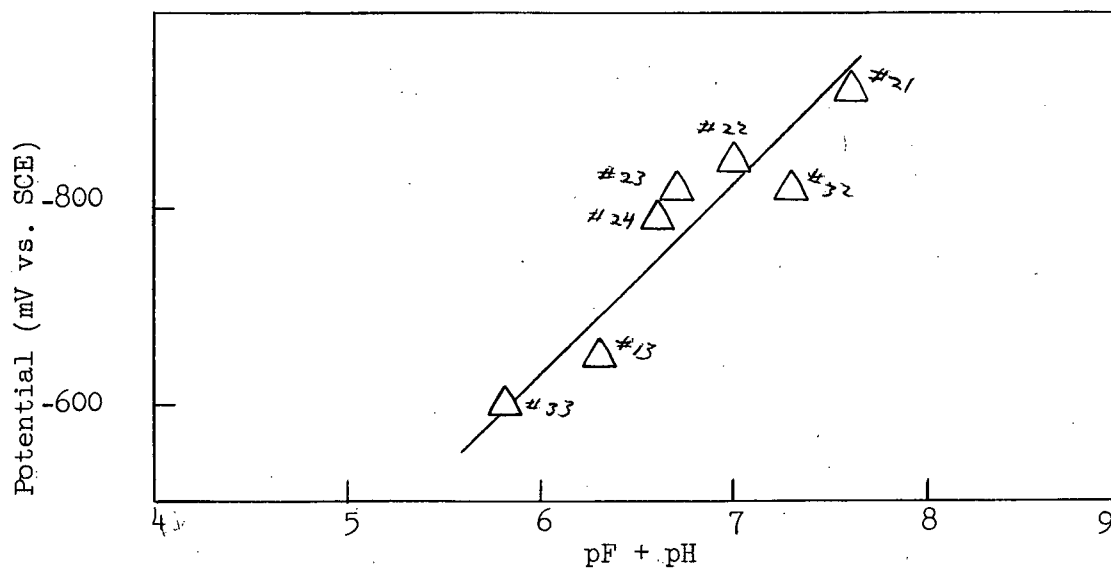
Figure 18. Potential at Second Active Peak versus pH plus pF.
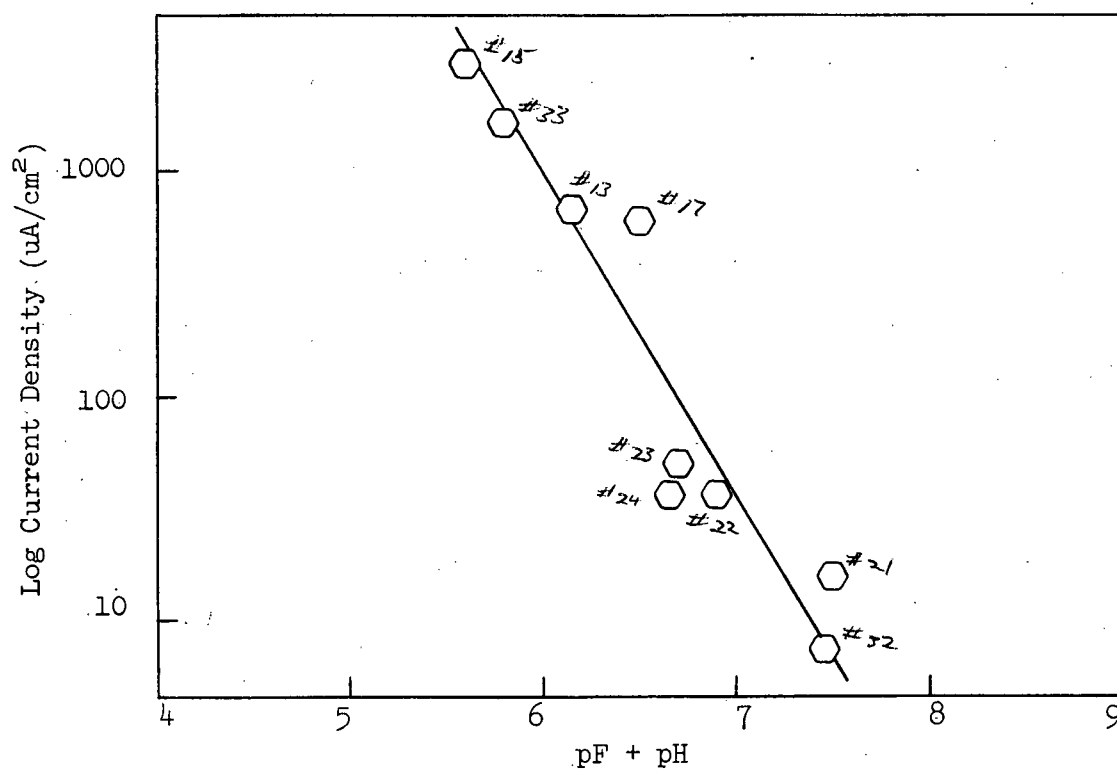
Figure 19. Log Current Density at the Second Active Peak versus pF plus pH.
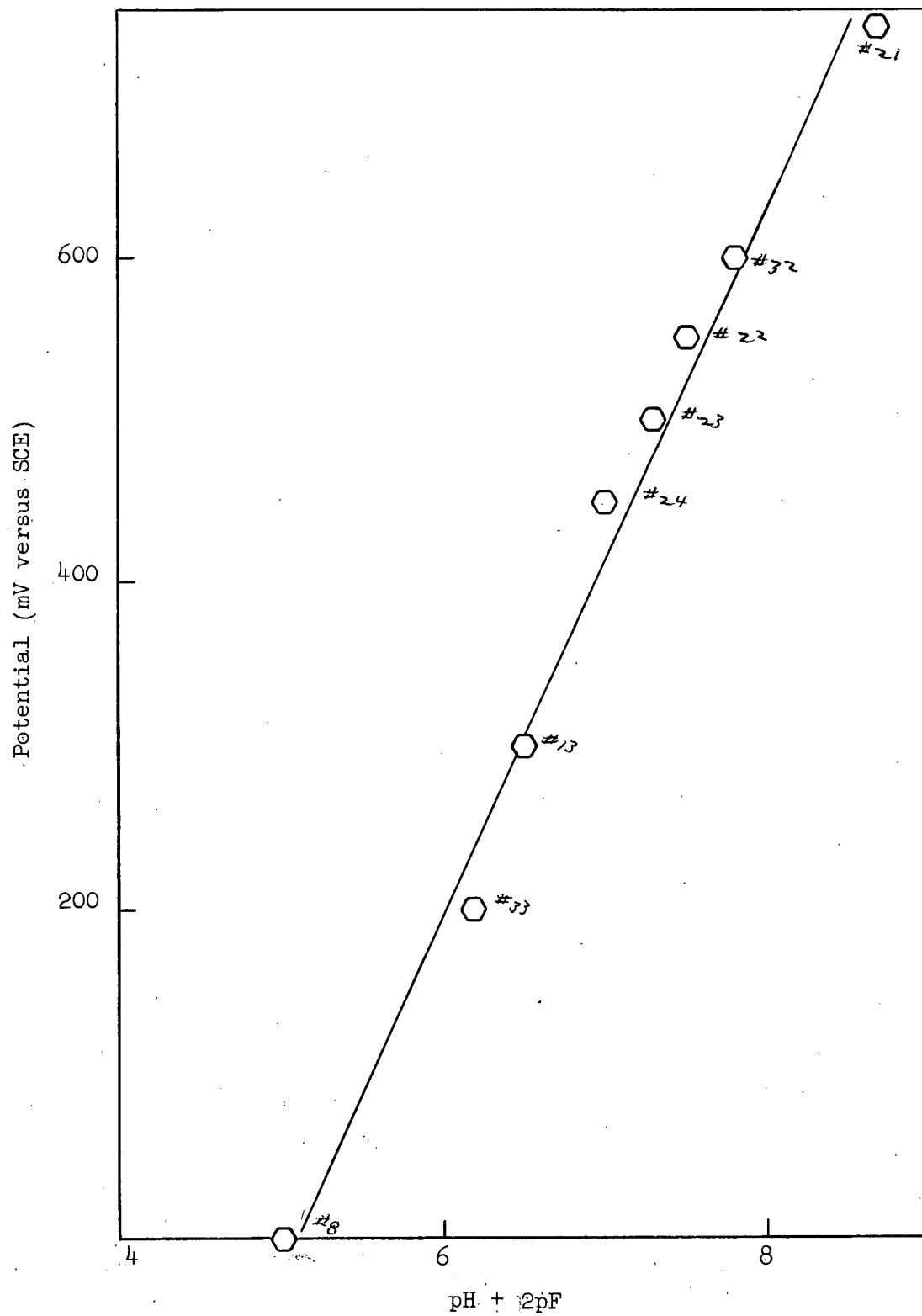
Figure 20. Potential at the Initiation of the
Second Active Region, E_c, versus
pH + 2pF.
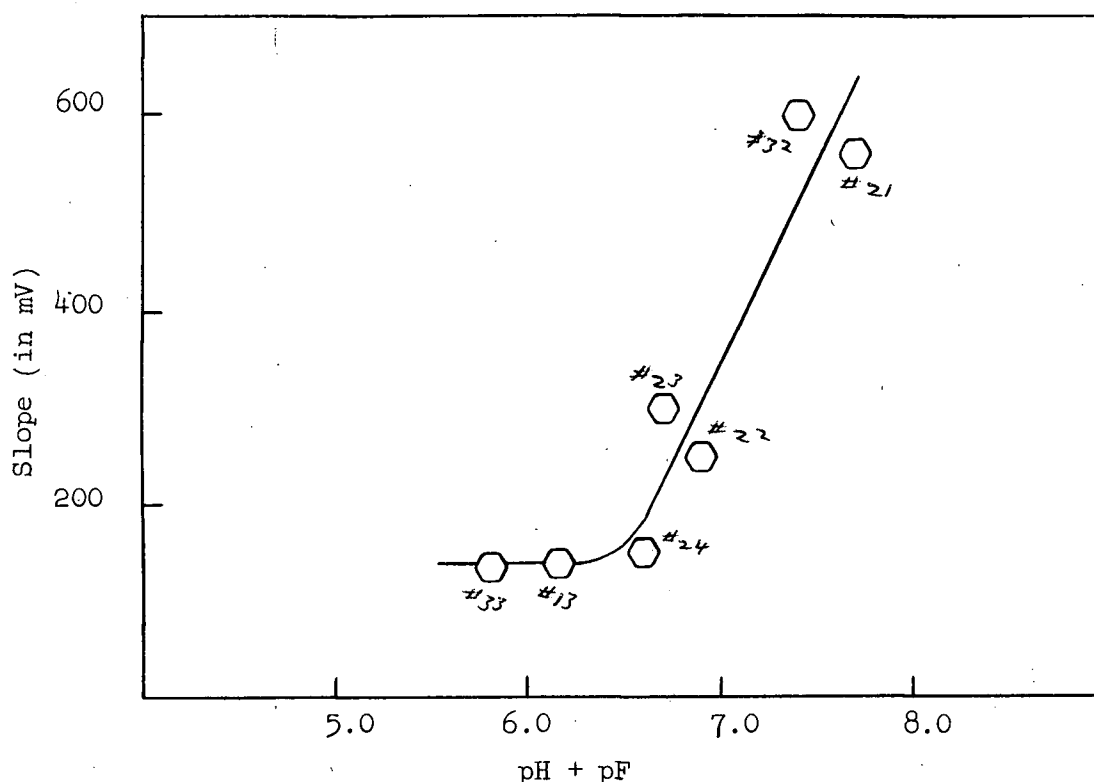
Figure 21. Positive Slope in Second Active Region versus
pH plus pF.

The second active region was absent in those two experiments
done in nitrate solutions with no fluoride ions present, as shown in Figure 11.
The minimum passive current was lower in these polarization curves but in
all other respects they resembled experimental curves for fluoride-containing
solutions. On the other hand 0.2 M chloride solutions, Figure 22, showed a
second active region in agreement with observations by other investigators[8].
This curve shows that smaller concentrations of chloride ions induce greater
corrosion rates than fluoride ions.

In fluoride solutions the nickel became passive again at potentials
more noble than about -950 mV. In chloride solutions this probable final
passive region was not observed because the current density in the second
active region was so much larger that it was impossible to polarize the electrode
to the potential of maximum current.
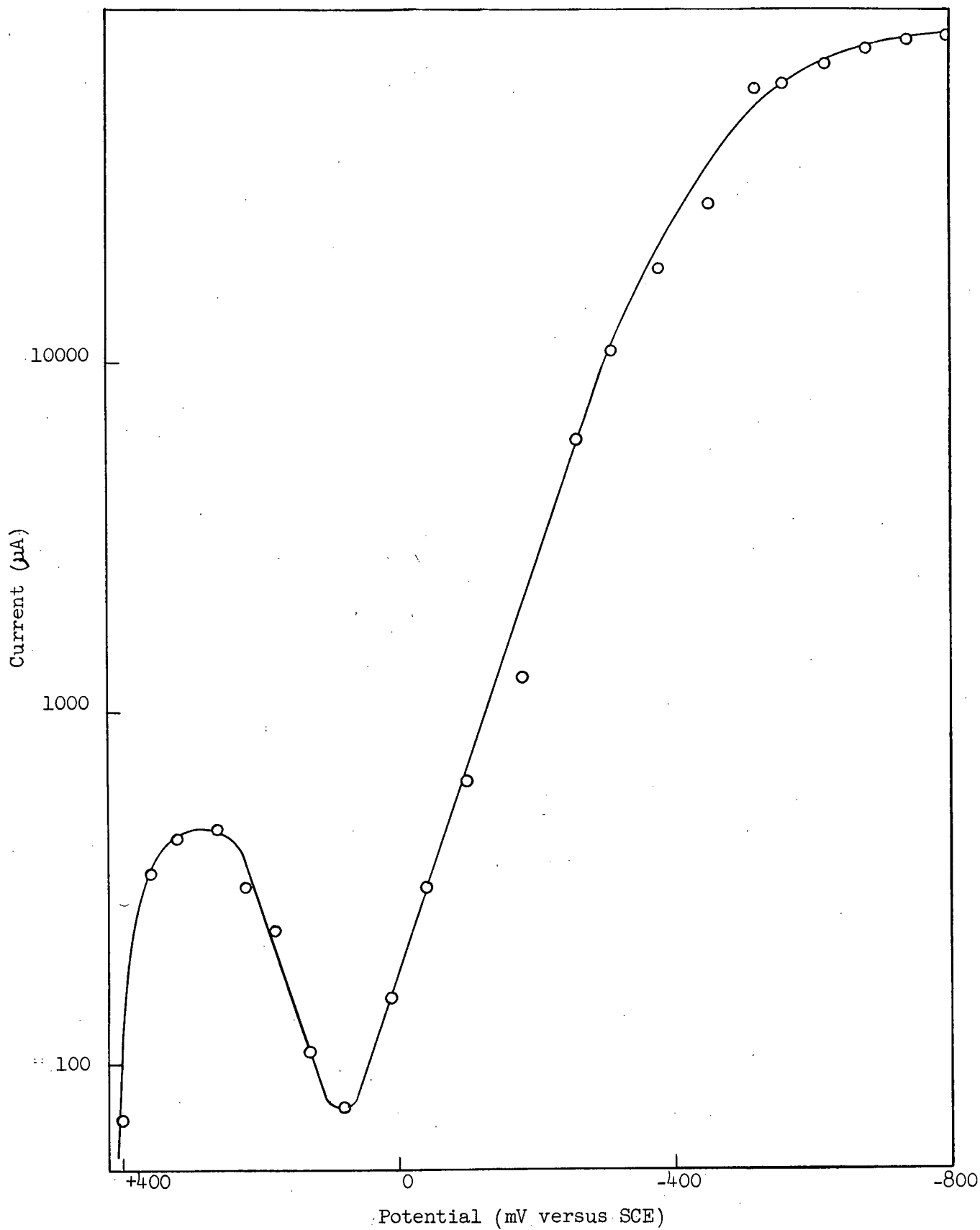
Figure 22. Polarization of Nickel in 0.2 M NaCl Solution at pH = 6.1 *Run #20*

Current-time curves at potentials in the region of secondary activation show initial decreases in current followed by a small rise, Figure 15. It is possible these represent film growth in passive areas in competition with the increasing area of the dissolution sites.

A photomicrograph of a specimen used in the time-current experiments, Figure 23a, shows that the dissolution sites are grain boundaries. Interference colours on binocular examination of the specimens are interpreted to indicate film growth between the grain boundaries. Corrosion between the grain boundaries is also apparent but this is similar to the corrosion of nickel in the passive region, Figure 17a.

Corrosion in the second passive region shows general corrosion over the whole surface with slight grain boundary etching, Figure 23b. This also is similar to the corrosion by fluorides in the first passive region.

Specimens polarized in sodium chloride solutions were extremely pitted.

The above observations indicate that nickel cannot be protected by anodic polarization in fluoride solutions with $[F^-] > 0.01$ and at pH < 6.5, because the second active region predominates at potentials where nickel would ordinarily be passive. At pH > 6.5 nickel is passive if no strong oxidizing agent is present. The corrosion current in the second active region at $[F^-] < 0.01$ M is small enough so that nickel could be protected at pH < 6.5 by anodic polarization, either applied by a chemical oxidant or by an external current.
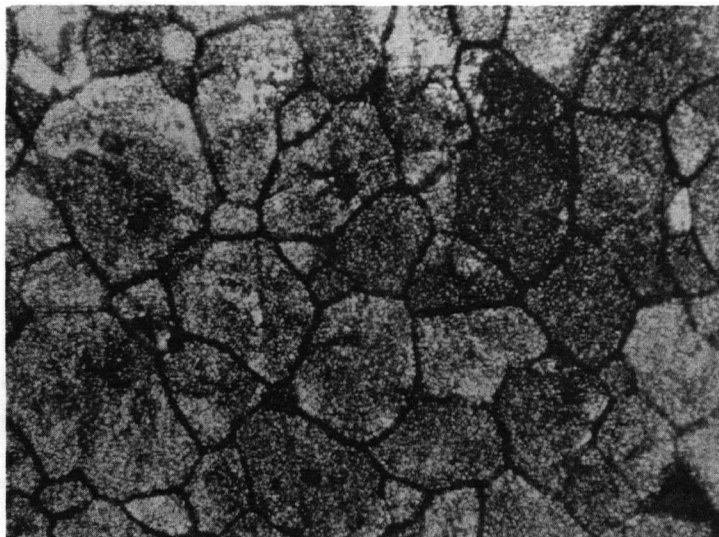
(a) At the second active peak, -700 mV

X 300

(b) In the second passive region, -1050 mV

X 300

Figure 23. Surfaces of Nickel Corroded in Fluoride Solutions
at pH = 6.2

Nickel in Basic Fluoride Solutions

The polarization curve, Figure 24, indicates that nickel is passive in contact with an aqueous solution of fluorides at high pH. This curve is an example of the type drawn in Figure 3(c) and would be predicted from the pH-potential diagram, Figure 5. (The small active peak in Figure 24 would probably be eliminated with longer times at constant potential).

If the film is assumed to be $Ni(OH)_2$, then the two reactions occuring on the surface of the electrode with no externally applied current are probably

$$2H^+ + 2e^- \longrightarrow H_2$$

and

$$Ni + 2OH^- \longrightarrow Ni(OH)_2 + 2e^-$$
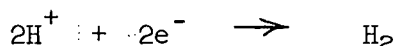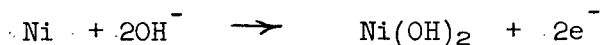
Thus the abrupt change in mixed potential as a function of pH (Figure 9) is explained by a change in the state of the oxidized nickel which would lead to a change in rate-control. In the active state the rate is controlled by the cathodic reaction as illustrated in Figure 4(b), whereas in the passive region the reaction is probably controlled by diffusion of the nickel ions through the oxide as in Figure 4(c).

The exchange current is very low (0.3 $\mu A/cm^2$) confirming that nickel is self-passivated in the pH range 6.5 to 12.0.

The first transpassive region is probably due to the formation of NiO_2. Kolotyrkin and Knyasheva[31] obtained the same behaviour with nickel in potassium sulphate solutions with a Tafel slope of 70 mV which compares very well with the value of 80 mV in this work. They explained the phenomena as due to the formation of NiO_2 on the electrode surface. Presumably the film would have a nickel defect lattice[28] and thus higher nickel ion conductivity.

The final rise in current at about -1200 mV is due to the evolution
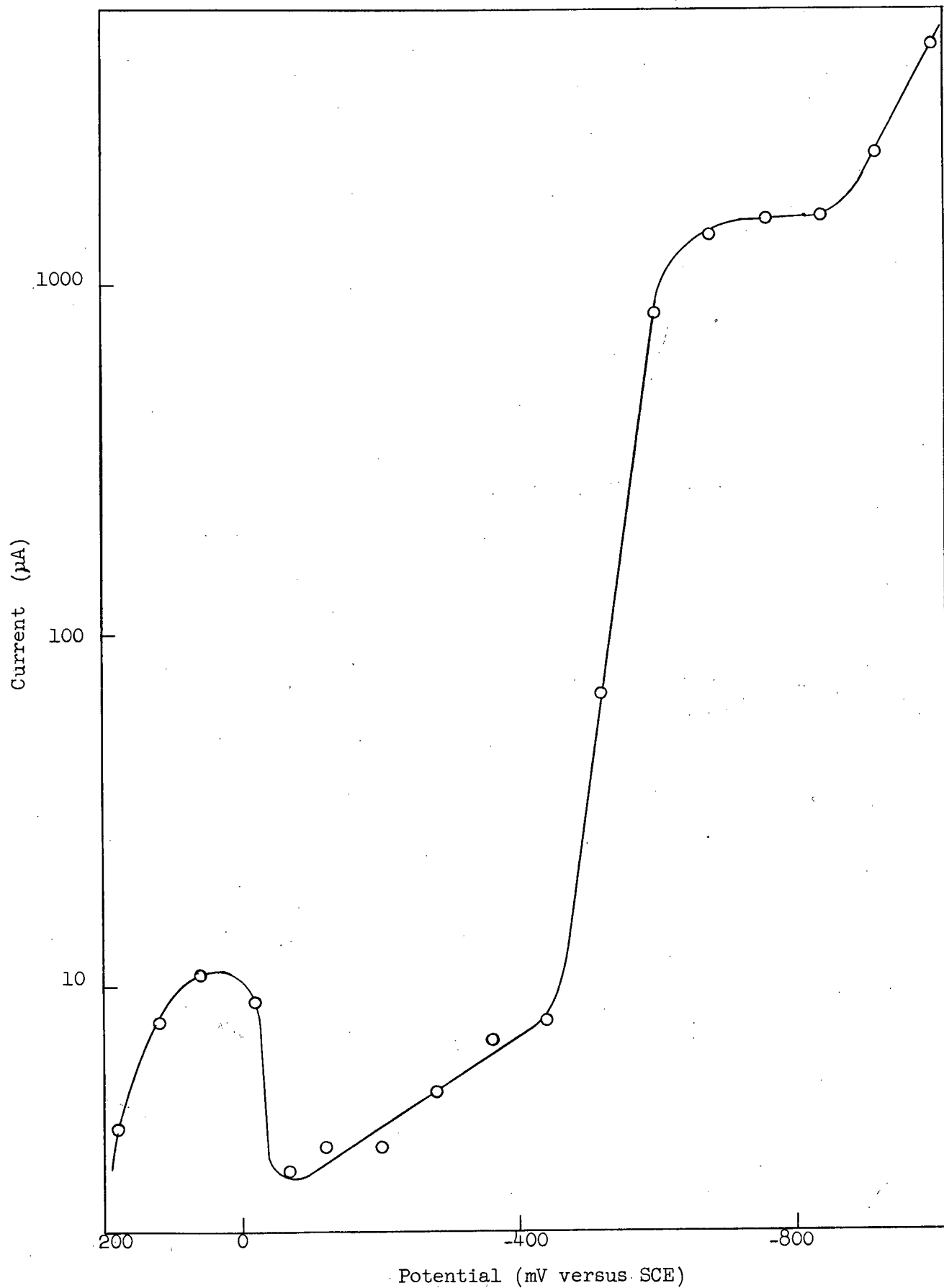
Figure 24. Polarization Curve for Nickel in 0.42 M NaF
Solution at pH = 11.3 *Run #10*

of oxygen and is not necessarily accompanied by rapid corrosion.

Mechanism of Nickel Corrosion in Fluoride Media

The mechanism whereby chloride ions in solution initiate a second active region on the polarization curve of zirconium, magnesium and aluminum has been proposed by Kolotyrkin[10]. The results on which this mechanism is based are very similar to the results obtained in the present work for nickel in fluoride and chloride solutions and the results of Truempler and Keller[8] for nickel in chloride and bromide solutions. The corrosion mechanism might therefore be expected to be the same in all cases.

Kolotyrkin's mechanism is based on the premise that halide ions adsorb on zirconium, etc, preferentially to hydroxide ions or water molecules at potentials above E_c, but not below, because of their greater polarizability. Chloride, bromide and iodide ions in fact have larger polarizabilities than either H_2O or OH^- (Table II) but fluoride ions have a smaller polarizability and nevertheless give rise to a similar though less extensive second active region. Therefore this mechanism must be invalid at least for corrosion by fluorides.

TABLE II.

Species	Polarizability $\alpha_o \times 10^{24} cm^3$	Gram Ionic Refraction R cm^3
F^-	0.99	2.60
Cl^-	3.02	9.03
Br^-	4.17	12.60
I^-	6.28	19.00
OH^-	1.80 �	5.10
$O^=$	2.76	-
H_2O	1.44	-

✷ Value extrapolated from Refractive Index.

A new mechanism is proposed that accounts for corrosion by all halide ions in the second active region.

The following mechanism is based on the premise that the surface

charge on nickel, zirconium etc. is negative at their reversible potentials[32].

The negative surface charge arises from the dissolution of positive metal

ions from an electrically insulated metal in solution thus leaving a negative

charge on the surface. This is called the electrolytic solution effect and

is opposed by the electrostatic attractive force, the force of attraction

between the dissolved positive ions and the surface, and the osmotic effect

which is effectively the sum of all other forces tending towards deposition

of the cations on the metal surface. The osmotic and electrostatic attractive

forces are considered to be greater than the electrolytic solution effect

only for very noble metals like platinum and gold, giving rise to a net

positive charge on the surface in such cases. Nickel is considered to be

active enough to maintain a negative charge on its surface at its reversible

redox potential producing a potential field at the metal-solution interface

of unknown value. Therefore, the electrode repulses negative ions at the

nickel-hydrogen mixed potential, which, in indifferent electrolytes, is close

to its reversible redox potential in the pH range considered, Figure 5. Only

water molecules would be adsorbed under these conditions. As the potential

of the electrode is made more noble, nickel ionizes more readily, hydrolyzing or

forming halide complexes away from the nickel surface. This gives rise to

the first active region in the polarization curve. Thus the corrosion mechanism

in this region is:

$$H_2O \longrightarrow H_2O_{ads} \qquad \qquad \ldots\ldots(1a)$$

$$Ni(H_2O)_{2ads} \longrightarrow Ni^{++}(H_2O)_2 + 2e^- \qquad \ldots\ldots(1b)$$

$$Ni^{++}(H_2O)_2 \longrightarrow Ni(OH)_2 + 2H^+ \qquad \ldots\ldots(1c)$$
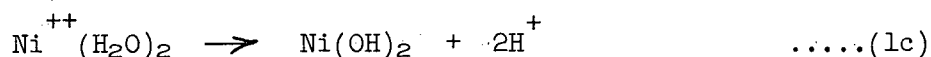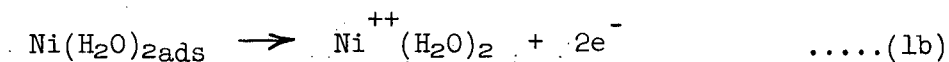
the last step occurring away from the surface. At even more noble potentials,

the electric field initiates hydrolysis of the oxidized nickel near the surface;

the more positive the charge on the surface, the closer to the surface is the hydrolysis reaction until it occurs close enough to form an adherent film on the electrode. This mechanism predicts the pH dependence of the Flade potential E_F, the potential at which the hydrolysis reaction results in an adherent film. As noted previously the data of the Flade potential as a function of pH fits the relation:

$$E_F = -0.240 + 0.065 \text{ pH} \qquad \qquad \dots\dots(2)$$

This mechanism also predicts that the first active region is independent of the fluoride ion concentration. This is confirmed by the results of the present work, Figures 12 and 13.

As the electrode surface is made more positive, the electric field attracts negatively charged ions such as OH^-, Cl^- and F^- which compete with water molecules for adsorption sites. This adsorption in aqueous fluoride solutions may be described quantitatively by the Langmuir adsorption isotherm,

$$\frac{\Theta_1}{1 - \Theta_1 - \Theta_2} = K_1 \ [F^-] \qquad \qquad \dots\dots(3)$$

where Θ_1 and Θ_2 are the proportions of the surface covered by fluoride and hydroxide ions, $1 - \Theta_1 - \Theta_2$ is the proportion of surface covered by water molecules, and K_1 is an equilibrium constant.

Kinetic considerations of adsorption and desorption show that

$$K_1 = k \ e^{\frac{\Delta H}{RT}} \qquad \qquad \dots\dots(4)$$

where k is a constant and ΔH is the enthalpy of adsorption. The enthalpy may be written:

$$\Delta H_1 = \Delta H_{O_1} - \beta \ n \ F \ E \qquad \qquad \dots\dots(5)$$

where ΔH_{O_1} is the standard enthalpy with no applied field, E is the applied field, n is the charge on the ion moving in the electric field, β is the proportion of the applied potential through which the ion moves when adsorbed, and F is the Faraday constant.
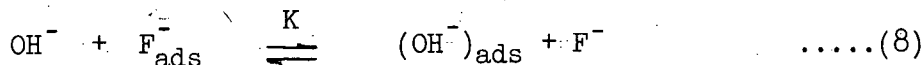
From this it follows that

$$\frac{\Theta_1}{1 - \Theta_1 - \Theta_2} = [F^-] \, k \, e^{\Delta H_{O_1} - \beta FE} \qquad \ldots\ldots(6)$$

A similar equation can be obtained for adsorption of hydroxide ions which when added to the above relation gives

$$\frac{\Theta_1 + \Theta_2}{1 - \Theta_1 - \Theta_2} = \left\{ [F^-] \, k_1 \, e^{\frac{\Delta H_{O_1}}{RT}} + [OH^-] \, k_2 \, e^{\frac{\Delta H_{O_2}}{RT}} \right\} e^{\frac{-\beta FE}{RT}} \qquad \ldots\ldots(7)$$

where Θ_1, Θ_2, $[F^-]$, $[OH^-]$ and E are considered variables.

However, the fluoride and hydroxide ions also compete with each other for adsorption sites,

$$OH^- + F^-_{ads} \xrightleftharpoons{K} (OH^-)_{ads} + F^- \qquad \ldots\ldots(8)$$

with

$$K = \frac{\Theta_2 \, [F^-]}{\Theta_1 \, [OH^-]} \qquad \ldots\ldots(9)$$

which with equation (7) yields

$$\frac{\Theta_1 \, (1 + K \frac{[OH^-]}{[F^-]})}{1 - \Theta_1 \, (1 + K \frac{[OH^-]}{[F^-]})} = \left\{ [F^-] \, e_1 + [OH^-] \, e_2 \right\} e^{\frac{-\beta FE}{RT}} \qquad \ldots\ldots(10)$$

$$\text{where } e_{1,2} = k_{1,2} \, e^{\frac{\Delta H_{O_{1,2}}}{RT}}$$

From this it follows that

$$e^{\frac{-\beta FE}{RT}} = \frac{\Theta_1 \, (1 + K \frac{[OH^-]}{[F^-]})}{[F^-]e_1 + [OH^-]e_2 - \Theta_1[F^-]e_1 - \Theta_1[OH^-]e_2 - K\Theta_1[OH^-]e_1 - K\Theta_1\frac{[OH^-]^2}{[F^-]}e_2}$$

$$\ldots\ldots(11)$$

The fourth and sixth terms in the denominator are negligible because K is considered large and $[OH^-]$ is in the order of 10^{-7} or less.

Thus, by ignoring these terms,

$$e^{-\frac{\beta FE}{RT}} = \frac{\theta_1 \left(\frac{1}{OH^-} + \frac{K}{[F^-]}\right)}{\frac{[F^-]}{[OH^-]} e_1 + e_2 (1 - K\theta_1)} \qquad \ldots\ldots(12)$$

and taking logarithms

$$-2.3 \frac{\beta FE}{RT} = \log \theta_1 + \log\left(\frac{1}{OH^-} + \frac{K}{F^-}\right) - \log\left\{ \frac{[F^-]}{[OH^-]} e_1 + e_2 (1 - K\theta_1) \right\} \qquad \ldots\ldots(13)$$

It may be assumed that a critical concentration of adsorbed fluoride ions is necessary to initiate the corrosion which results in the second active region on the polarization curve and thus θ_1 may be considered a constant, θ_1 crit. Four limiting cases are considered to ascertain the pH and pF dependence of E_c, the potential at the initiation of the second active region. In case 1 it is assumed that $\frac{1}{[OH^-]} \gg \frac{K}{[F^-]}$ and $(1 - K\theta_1)e_2 \gg \frac{[F^-]e_1}{[OH^-]}$. This results in the relation:

$$-2.3 \frac{\beta F}{RT} E_c = \log \theta_1 \text{ crit } - pH - \log (1 - K\theta_{crit}). \qquad \ldots\ldots(14)$$

which shows no dependence of E_c on fluoride concentration and therefore is inconsistent with experimental evidence. Case 2 applies when $\frac{1}{[OH^-]} \gg \frac{K}{[F^-]}$ and $\frac{[F^-]}{[OH^-]} e_1 \gg (1 - K\theta_1)e_2$ and yields

$$-2.3 \frac{\beta F}{RT} E_c = \log \theta_1 \text{ crit } - \log e_1 + pF \qquad \ldots\ldots(15)$$

This shows no dependence of E_c on pH and is also inconsistent with experiment. Similarly, case 3, $\frac{K}{[F^-]} \gg \frac{1}{[OH^-]}$ and $(1 - K\theta)e_2 \gg \frac{[F^-]}{[OH^-]}$ yields no pH-dependence and may be disregarded. Case 4, $\frac{K}{[F^-]} \gg \frac{1}{[OH^-]}$ and

$$\frac{[F^-]}{[OH^-]} \quad e_1 \quad >> \quad (1 - K \Theta) e_2 \quad \text{results in the expression}$$

$$-2.3\frac{\beta F}{RT} E_c = \log \Theta_{1 \text{ crit}} + \log K + pF - \log e_1 + pF + pH \qquad \ldots\ldots(16)$$

in which E_c is a function of $pH + 2pF$. This is in accordance with the experimental results, Figure 20, and may be rationalized by considering K very large. The above expression, when written in the form

$$E_c = C + \frac{RT}{2.3\beta F} \log \Theta_{1 \text{ crit}} - \frac{RT}{2.3\beta F}(pH + 2pF) \qquad \ldots\ldots(17)$$

indicates that a plot of E_c versus pH plus 2pF would have a slope of $\frac{RT}{2.3\beta F}$ or $\frac{59.1}{\beta}$ mV. In Figure 20 the slope is approximately 230 mV which agrees with that predicted for the above mechanism if $\beta = 0.26$. The energy of adsorption is only a proportion of the total energy of an ion moving through the total applied potential, as illustrated in Figure 25.
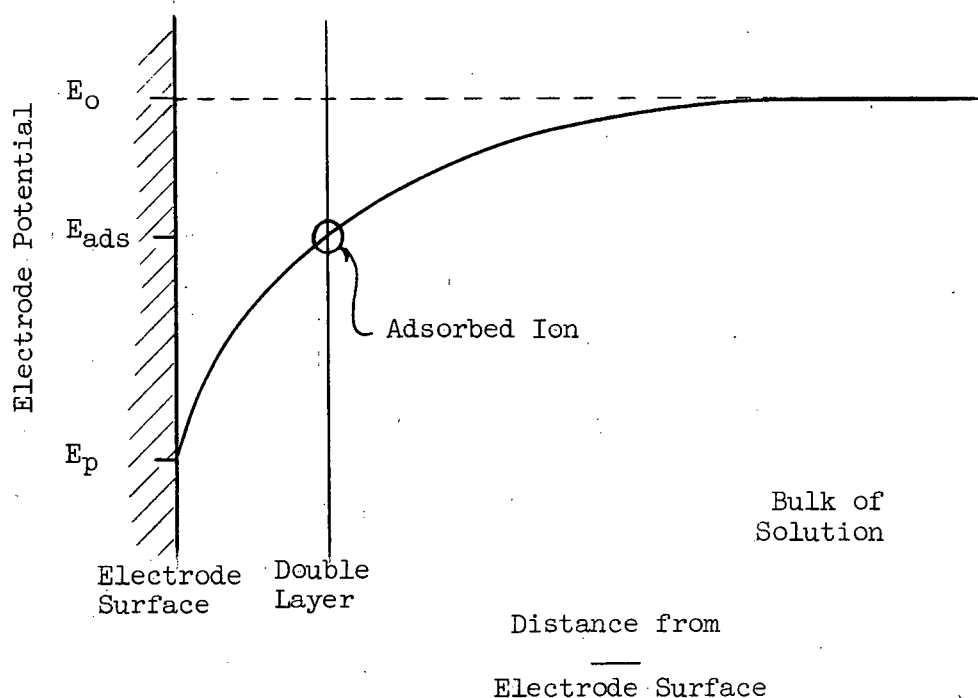

Figure 25. Potential Function of Ion in Vicinity of a Charged Electrode

β is defined as the change in the energy of adsoption with change in the applied potential (i.e. $\beta = \dfrac{E_{ads}}{E_{applied}}$).

Adsorption of fluoride ions occurs at relatively active potentials if pH and pF are small, that is, if there is small hydroxide ion and large fluoride ion concentration as predicted by equation (17) Recent work[33] with platinum in chloride solutions has shown that adsorption of chloride ions is favoured by low pH and large chloride ion concentrations. It was also found that chloride adsorption inhibits coverage of the surface by adsorbed oxygen.

Adsorption of fluoride ions can be expected to occur at weak spots in the nickel hydroxide film. In such places as grain boundaries and dis-location sites, the metal is probably slowly dissolving. As fluoride ions carry   current to these sites, fluoride adsorption will occur there most rapidly. In the present work, nickel sulphide has been identified at the grain boundaries, Figure 26. Any passivating film is likely to be particularly weak on the sulphide phase and therefore corrosion will be initiated pre-ferentially at the grain boundaries.
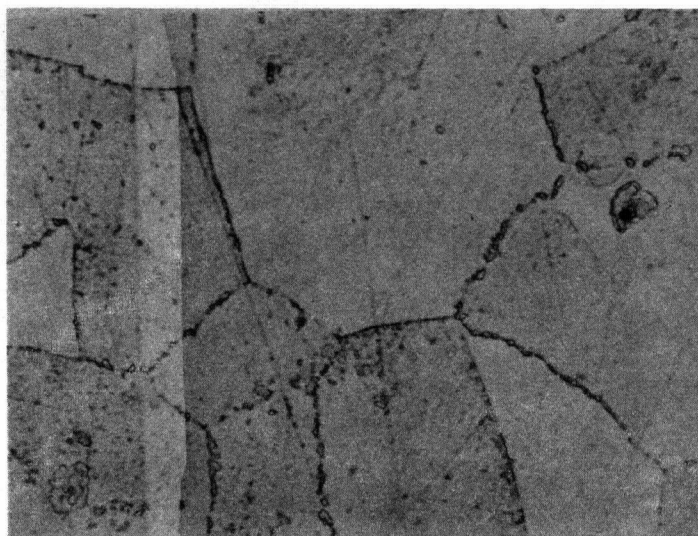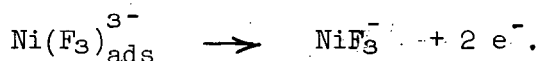
Figure 26. Micro-structure of Nickel Showing Second Phase.

The adsorbed fluoride ions will form a soluble nickel-halide complex, probably NiF_3^-, and thus initiate a corrosion reaction. The mechanism is

$$Ni(H_2O)_{n_{ads}} + 3F^- \longrightarrow Ni(F_3)^{3-}_{ads} + n\ H_2O$$

$$Ni(F_3)^{3-}_{ads} \longrightarrow NiF_3^- + 2\ e^-.$$

Halide ions carry part of the current to these sites and thus maintain a sufficient concentration for the reaction to proceed at these localized sites, grain boundaries in this case, Figure 22a.

The increase in current with potential will fit the Tafel equation if the rate-control is activation of the nickel oxidation step. This is the case at large fluoride ion concentrations and low pH (Figure 21). The slope 135 mV, indicates an oxidation process in which one electron at a time is exchanged. At higher pF and pH hydroxide adsorption interferes and the rate is controlled by competition between the two adsorbing anions. At high pF and low pH the rate may also be controlled by diffusion of the fluoride ions to the site.

The above mechanism which gives rise to the second active region in neutral solutions can be applied to corrosion processes at anodic potentials up to -800 mV in acid fluoride solutions, (Figure 8). The plots of the Flade potential and the critical halide adsorption potential versus pH show that fluoride ions adsorb at more active potentials than the Flade potential at pH = 3.5 Figure 27. Additional support is found in Figure 10a, which shows extensive grain boundary corrosion on a specimen subjected to corrosion at anodic potentials in acid fluorides, apparently identical with corrosion in the second active region in neutral solutions (Figure 27). Thus nickel corrodes
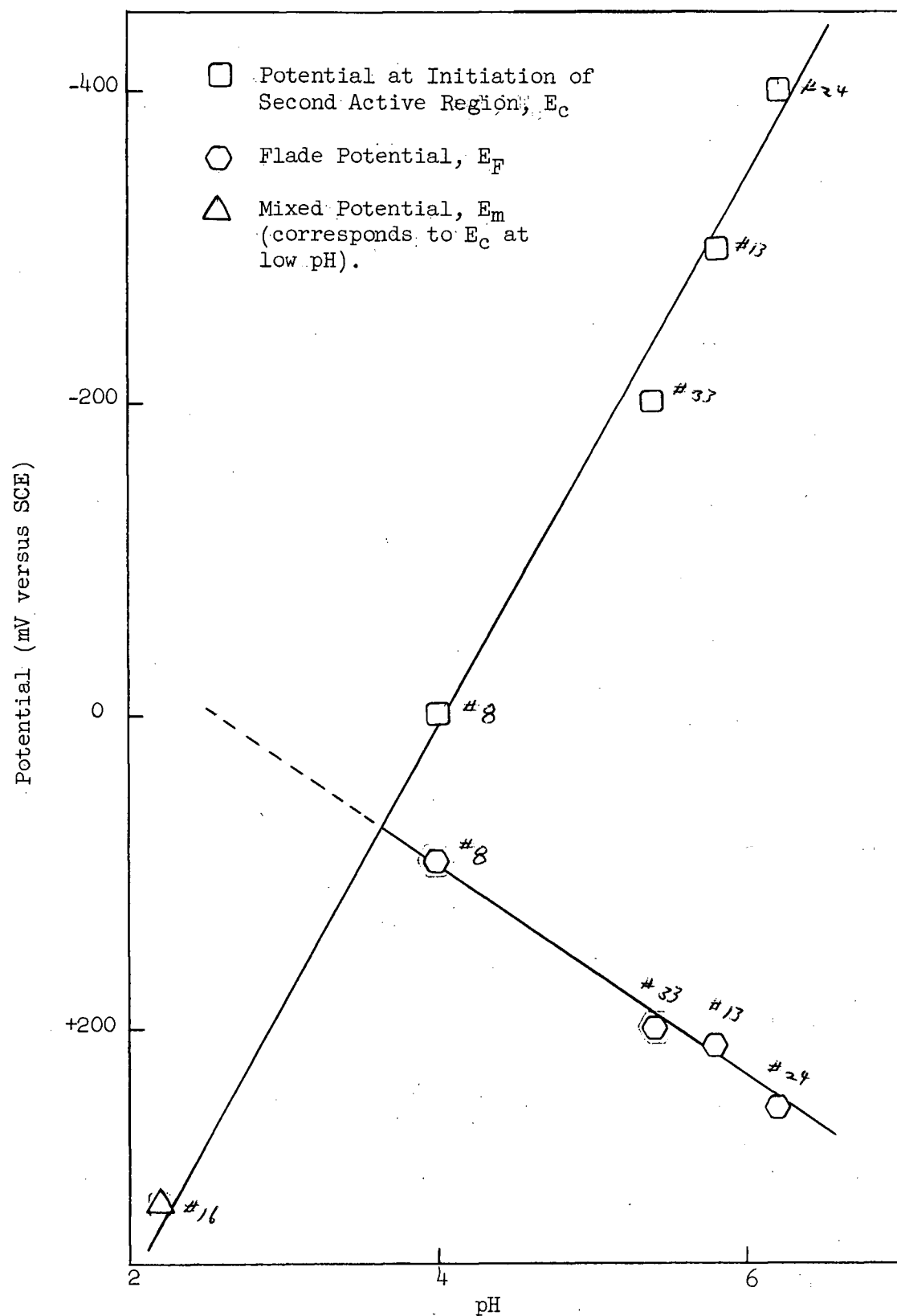
Figure 27. Flade Potential, E_F, and Potential at Initiation of Second Active Region versus pH

in low pH solutions at all anodic potentials by complexing with fluoride
ions.

The gradually sloping polarization curve at noble potential in
acid fluoride solutions indicates that the rate is controlled by mixed
concentration polarization and diffusion of fluoride ions to the dissolution
sites. Since these sites are specific, the anions must travel partly
perpendicular to the potential field. This part of their movement will
be potential independent and gives rise to a larger Tafel slope.

The polarization curve for nickel in neutral fluoride solutions
shows that nickel is passive at potentials between -950 and -1100 mV.
Kolotyrkin[10] has suggested that oxygen preferentially adsorbs to metal
atoms with bonds corresponding to their highest oxidation state. This
reaction can be expected to occur as the electrode potential is made more
positive and therefore displaces halide ion adsorption. Iron is known to
dissolve from pit sites as divalent ions and from passive areas as tri-
valent ions, in chloride and bromide solutions[29]. In addition, the pH-
potential diagram (Figure 5) predicts that Ni_2O_3 would form at potentials
more noble than -750 mV in the absence of halide ions. The second passive
region for nickel is therefore concluded to result from oxygen adsorption
to nickel to form a trivalent oxide film which is stable even in the presence
of halide ions.

Monel

Polarization studies on monel in fluoride solutions buffered at pH = 4.0, 6.2 (Figure 28) and 11.3 showed behaviour similar to nickel. However, monel has a higher overvoltage for the cathodic reaction:

$$2H^+ + 2e^- \longrightarrow H_2$$
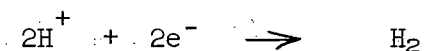
The resulting exchange currents are lower than for nickel (see Table III).

TABLE III.

Exchange Current for Monel and Nickel in Similar Solutions

pH	Monel	Nickel
4.0	6 uA/cm^2	16 uA/cm^2
6.0	2 uA/cm^2	8 uA/cm^2
11.0	0.3 uA/cm^2	0.6 uA/cm^2

These data indicates that monel is more resistant than nickel to fluorides in acid solution[5]. The exchange or corrosion current of monel in fluorides is controlled by the cathodic reaction as illustrated in Figure 4(b). Any environmental change which increases the rate of the cathodic reaction will increase the corrosion of monel.

At pH = 4 monel does not passivate in the presence of fluorides. The shape of the anodic curve is very similar to the anodic curve for nickel in fluorides at low pH.

In neutral fluoride solution, pH = 6 the anodic current decreases slightly on raising the potential past the active peak, Figure 28. The "passive" current was about 12 $\mu A/cm^2$ as compared to 2 $\mu A/cm^2$ for nickel.
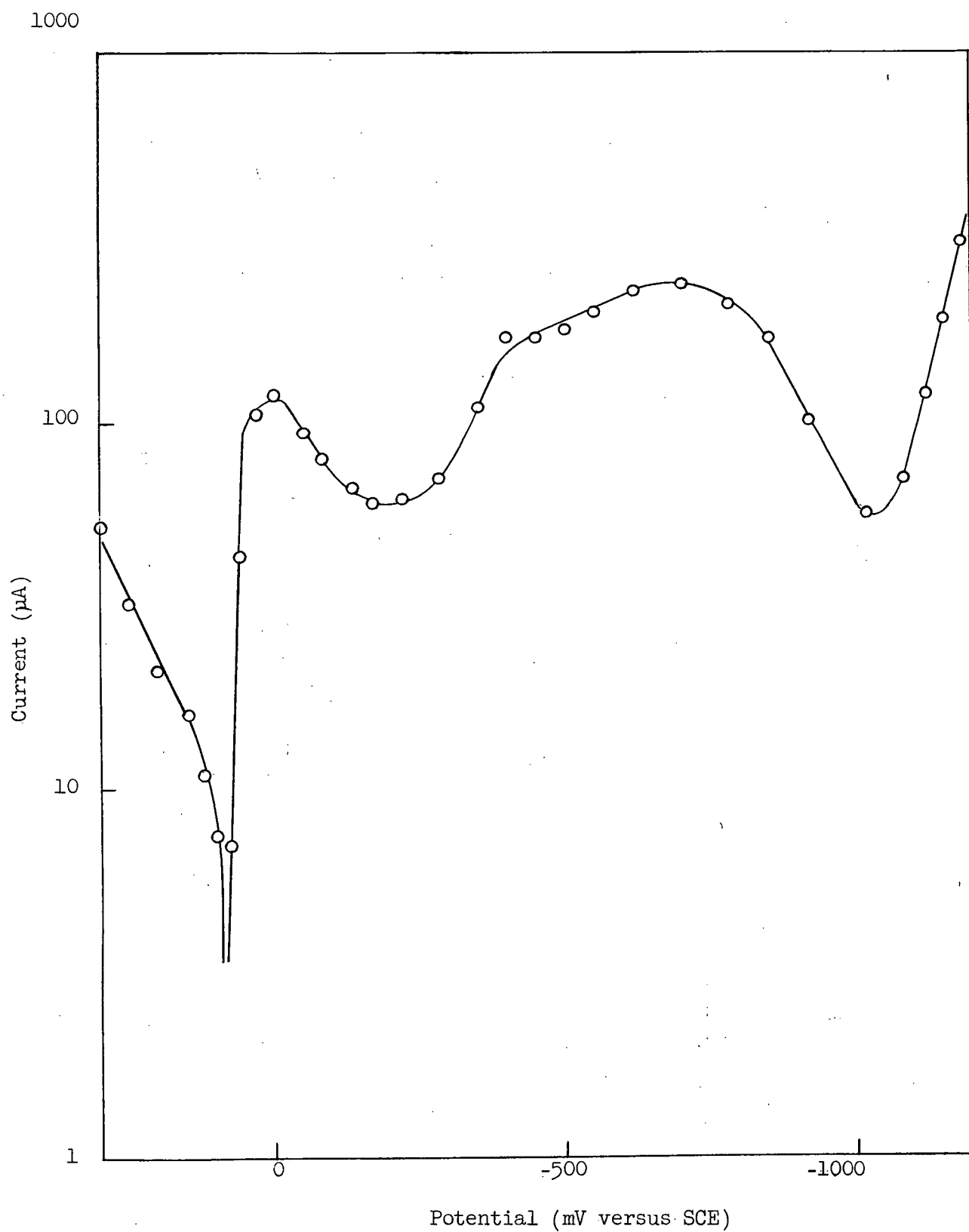
Figure 28. Polarization Curve of Monel in 0.42 M NaF Solution at pH = 6.0 *Run #28*

At higher pH, monel behaves similarly to nickel but again the "passive" current density is much larger. The exchange current is about 0.6 $\mu A/cm^2$ and the first active region is missing. The first transpassive region starts at a potential of -700 mV compared to -600 mV for nickel.

Optical examination of the specimens showed more pitting and large cavities.

No experiments to ascertain time dependence of the current at a fixed potential were done.

Monel was also polarized in chloride solution at pH = 6, Figure 29. The resulting curve was very similar to that obtained for nickel in chlorides but with a decreased Tafel slope in the second active region, 75 mV as compared to 180 mV for nickel.

Alloying copper to nickel produces a larger hydrogen overvoltage and this accounts for the lower exchange current. However, it also reduces the extent of passivation at more noble potentials. This may be caused by breakdown of the film due to copper dissolution. Arai[23] has found that in nickel-copper alloys containing more than about 50% copper, film breakdown occurs due to the formation of CuO at a faster rate than $Ni(OH)_2$. Uhlig has indicated that increases in copper content increase the "passive" current of nickel-copper alloys when polarized in sulphuric acid. He explains the decrease in the resistance as a result of the filling of the nickel d-orbitals by electrons from copper which is not a transition element. This decreases the susceptability of the alloy to oxygen adsorption and therefore decreases its ability to passivate.
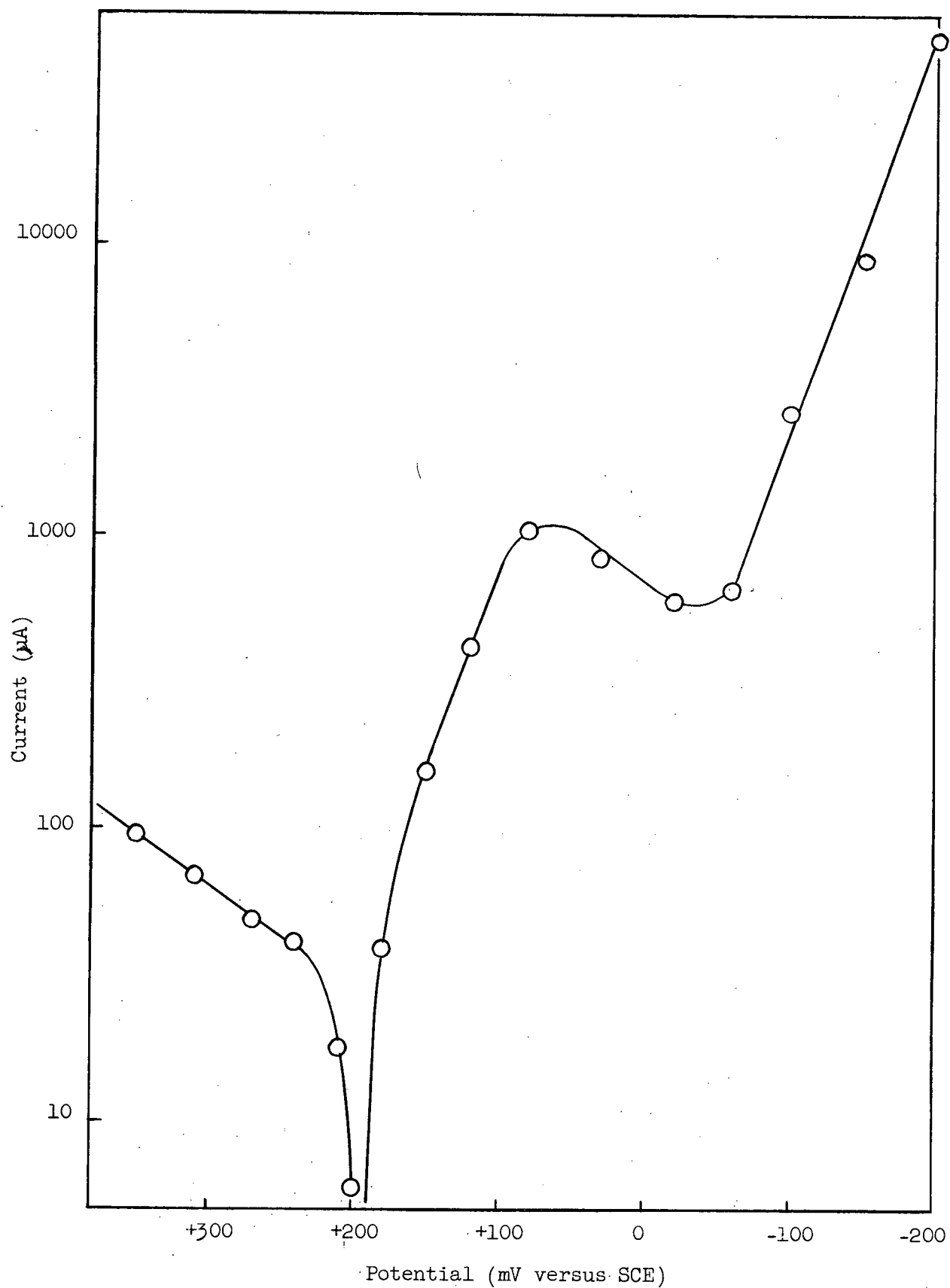
Figure 29. Polarization Curve of Monel in 0.42 NaCl
Solution at pH = 4.0   Run #31

CONCLUSIONS

1.   Nickel does not passivate in acid fluoride solutions and is preferentially corroded at the grain boundaries at anodic potentials up to -800 mV (versus SCE).

2.   The polarization curve for nickel in neutral fluoride solutions shows an active region at anodic potentials slightly above the mixed potential. Nickel is thought to corrode by forming aquo-complexes in this region in which fluoride ions have no effect.

3.   Nickel becomes passive in neutral solutions at potentials E_F, according to the relation

$$E_F = -0.240 + 0.065 \text{ pH}$$

by hydrolysis of the aquo-complexes at the surface to form an adherent hydroxide film. Fluoride ions in solution increase the corrosion current in the passive region.

4.   Fluoride ions in neutral solution initiate a second active region on the nickel polarization curve at potentials which are more active with increasing fluoride ion and decreasing hydroxide ion concentrations. A mechanism is proposed whereby the corrosion is initiated by the adsorption of fluoride at sufficiently noble potentials. These ions compete with hydroxide ions so that by considering the Langmuir adsorption isotherm, a relation between the critical halide adsorption potential, E_c, and pH and pF (the negative logarithm of fluoride ion concentration),

$$E_c = C - \frac{RT}{F} \ (\log \theta_{1 \text{ crit}} + \text{pH} + 2\text{pF})$$

is derived. The mechanism for corrosion in the second active region is

$$Ni(H_2O)_{n_{ads}} + 3F^- \longrightarrow Ni(F_3)_{ads}^{3-} + n \ H_2O$$

$$Ni(F_3)_{ads}^{3-} \longrightarrow NiF_3^- + 2e^-$$
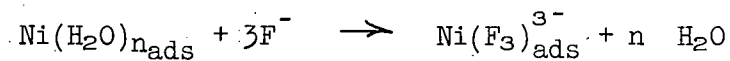
5. Nickel becomes passive at potentials more noble than -950 mV in neutral fluoride solutions, probably due to the formation of a passive film(Ni_2O_3 or higher oxide).

6. Nickel is passive in contact with fluoride solutions with $6.5 < pH < 12$.

7. Monel corrodes less rapidly at the mixed potential in aqueous fluoride solutions because of its higher hydrogen overvoltage. However, at anodic potentials, monel does not really passivate.

8. Nickel and monel corrode more rapidly in chloride solutions than in fluoride at all anodic potentials.

RECOMMENDATIONS FOR FUTURE INVESTIGATIONS

1.   The corrosion of nickel in fluoride media could be studied as a function of temperature to establish the temperature range over which the corrosion mechanisms may be applicable, and to obtain more detailed thermodynamic relationships.

2.   Polarization studies of nickel in solutions of chloride, bromide and iodide would reveal the extent to which the mechanism for corrosion by fluorides in the second active region applies to other halide ions.

3.   Polarization techniques in which a square wave alternating current is superimposed on the applied potential are useful in determining the properties of the passivating film and the double layer. These may be applied to nickel corrosion in halide solutions, expecially in passive regions.

4.   Corrosion studies of metals such as zirconium, aluminum, and magnesium in fluoride solutions to establish the relationships of corrosion mechanisms on these metals (which were found to yield a second active region in chloride) to the mechanisms of nickel corrosion, would be valuable.

REFERENCES

1.   G. C. Whittaker, Corrosion, 6, 283 (1950).

2.   F. Maness, U.S. Atomic Energy Comm. Report HW-68426 (1961).

3.   J. Bergman and G. W. C. MacDonald, Corrosion, 17, 9 and 12 (1961).

4.   E. I. Antonovskaya and L. V. Takhtarova, Zhur. Vsesoyuz. Khim. Obshchestva im D. I. Mendeleeva, 6, 477 (1961). (C.A. 56:292g)

5.   M. Schussler, Ind. Eng. Chem. 47, 133 (1955).

6.   W. J. Braun, F. W. Fink and G. Lee Erickson, U.S. Atomic Energy Comm. Report BMI-1237 (1957).

7.   D. R. Turner, J. Electrochem. Soc., 98, 434 (1951).

8.   G. Truempler and R. Keller, Helv. Chim. Acta 44, 1691 (1961).

9.   Y. Kolotyrkin and G. W. Gilman, Dokl. Akad. Nauk. SSSR, 137, 642 (1961).

10.   Y. Kolotyrkin, "First International Congress on Metallic Corrosion" 1961, Butterworths, London, 1962, p. 10.

11.   L. Tronstad, Trans. Faraday Soc. 29, 502 (1933).

12.   D. H. MacGillavry, J. H. Rosenbaum and R. W. Stevenson, J. Electrochem. Soc. 89, 22 (1952).

13.   K. J. Vetter and K. Arnold, Z. Elektrochem., 64, 244 (1960).

14.   J. Osterwald and H. H. Uhlig, J. Electrochem. Soc., 108, 515 (1961).

15.   U. R. Evans, "First International Congress on Metallic Corrosion" 1961, Butterworths, London, 1962, p. 3.

16.   N. Ya. Bune and Y. Kolotyrkin, Zhur. Fiz. Khim, 35, 1543 (1961).

17.   N. D. Greene, Corrosion, 15, 369 (1959).

18.   M. Stern and A. L. Geary, J. Electrochem. Soc., 104, 56, 559 and 645 (1957).

19.   M. Stern, Corrosion, 14, 440t (1958).

20.   W. A. Mueller, Corrosion, 18, 349 (1962).

21.   V. Chikal and M. Prazak, J. Iron and Steel Inst. 193, 360 (1959).

22.   T. P. Hoar, J. Appl. Chem., 11, 121 (1960).

23.   N. D. Greene, Corrosion, 18, 136t (1962).

24.	T. P. Hoar, "Anodic Behaviour of Metals" in "Modern Aspects of Electrochemistry", II, ed. J. O'M. Bockris, Butterworths, London, 1959, p. 272.

25.	Ibid, p. 325.

26.	R. Littlewood, Corrosion Science 3, 99 (1963).

27.	M. Pourbaix, "Atlas D'Equilibres Electrochimiques", Gauthier-Villars, Paris, p. 333, (1963).

28.	Arai Yoshi, Kogyo Kagaku Zasshi, 64, 600 (1961).

29.	J. L. Weininger and W. R. Grams, J. Electrochem. Soc. 109, 984 (1962).

30.	U. F. Franck, "First International Congress on Metallic Corrosion", 1961, Butterworths, London, 1962, p. 113.

31.	Y. Kolotyrkin and V. M. Knyasheva, Zhur. Fiz. Chim. 30, 1990 (1956).

32.	R. J. Hartman, "Colloid Chemistry", Houghton Mifflin Company, Cambridge, 1947, p. 222-229.

33.	N. Hackerman and M. C. Banta, J. Electrochem. Soc. 111, 114 (1964).

APPENDIX A.

Potential Standardization

The standard calomel reference electrode used in all of the experiments was checked against the cadmium-cadmium sulphate half-cell.

A 99.999% cadmium electrode was fitted in the working electrode holder after ageing in sulphuric acid. A 0.907 molar cadmium sulphate solution was introduced into the cell and saturated with nitrogen. The potential between the reference electrode and cadmium electrode was read on the Pye potentiometer after 30 minutes and 60 minutes to be 680 mV.

The standard electrode potential of

$$Cd \longrightarrow Cd^{++} + 2e^-$$
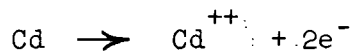
is 0.403 volts on the hydrogen scale as reported in Latimer[*]. Using an activity coefficient of 0.05, and the Nernst equation

$$E = E_O - \frac{RT}{nF} \ln \frac{[Cd^{++}] \; Cd^{++}}{[Cd]}$$

the electrode potential for the above system was 0.433 volts versus the hydrogen electrode or 0.684 versus the saturated calomel.

The experimental value of 0.680 volts is well within experimental accuracy.

---

[*] Latimer, W. M., "Oxidation Potentials", Englewood Cliffs, Prentice Hall, 1952.